

Variational Bayes for high-dimensional proportional hazards models with applications within gene expression

Michael Komodromos¹, Eric Aboagye², Marina Evangelou^{1,†},
Sarah Filippi^{1,†}, Kolyan Ray^{1,†}

¹Department of Mathematics, Imperial College London and,

²Department of Surgery and Cancer, Imperial College London

Abstract

Few Bayesian methods for analyzing high-dimensional sparse survival data provide scalable variable selection, effect estimation and uncertainty quantification. Such methods often either sacrifice uncertainty quantification by computing maximum a posteriori estimates, or quantify the uncertainty at high (unscalable) computational expense. We bridge this gap and develop an interpretable and scalable Bayesian proportional hazards model for prediction and variable selection, referred to as SVB. Our method, based on a mean-field variational approximation, overcomes the high computational cost of MCMC whilst retaining useful features, providing a posterior distribution for the parameters and offering a natural mechanism for variable selection via posterior inclusion probabilities. The performance of our proposed method is assessed via extensive simulations and compared against other state-of-the-art Bayesian variable selection methods, demonstrating comparable or better performance. Finally, we demonstrate how the proposed method can be used for variable selection on two transcriptomic datasets with censored survival outcomes, and how the uncertainty quantification offered by our method can be used to provide an interpretable assessment of patient risk.

Availability and implementation: our method has been implemented as a freely available R package `survival.svb` (<https://github.com/mkomod/survival.svb>).

Contact: mk1019@ic.ac.uk

[†]Equal contribution

Accepted in Bioinformatics <https://doi.org/10.1093/bioinformatics/btac416>

1 Introduction

The development of high-throughput sequencing technologies has led to the production of large-scale molecular profiling data, allowing us to gain insights into underlying biological processes (Widlak, 2013). One such technology is microarray sequencing, in which mRNA counts are used to describe gene expression. Such data, known as transcriptomics, are widely used in the biomedical domain and when analyzed alongside survival times have provided extraordinary opportunities for biomarker characterization and prognostic modelling (Bøvelstad et al., 2007; Lloyd et al., 2015; Lightbody et al., 2019; Lu et al., 2021). However, profiling data is often high-dimensional, which introduces several statistical challenges including: (i) variable selection, (ii) effect estimation of the features, (iii) uncertainty quantification, and (iv) scalable computation. The task of variable selection is particularly important, as few genes typically have an effect on the outcome. Motivated by clinical applicability, we propose a state-of-the-art scalable (variational) Bayesian variable selection method for the proportional hazards model.

In recent years, several methods have been proposed to analyze sparse high-dimensional data, with one of the most popular being the LASSO (Tibshirani, 1996). As biomedical studies are often concerned with clinical phenotypes, such as time to disease recurrence or overall survival time, these methods have been adapted to support survival analysis (Antoniadis et al., 2010; Witten and Tibshirani, 2010). For instance, the LASSO, ridge and elastic-net penalties have all been extended to the proportional hazards model (Tibshirani, 1997; Gui and Li, 2005; Zou and Hastie, 2005; Simon et al., 2011). More recently, Bayesian shrinkage and variable selection methods have grown in popularity (Park and Casella, 2008; O’Hara and Sillanpää, 2009; Carvalho et al., 2010; Li and Zhang, 2010; Bhadra et al., 2019; Lewin et al., 2019; Bai et al., 2021), with several methods being extended to survival data (Tang et al., 2017; Maity et al., 2020; Nikooienejad et al., 2020).

Bayesian approaches to variable selection are popular, not least since the relevance of a covariate can be assessed simply by computing the posterior probability that it is included in a model. This recasts variable selection as a model selection problem (Mitchell and Beauchamp, 1988; George and McCulloch, 1993), with every possible model assigned an individual posterior probability. One of the most popular such model selection priors is the spike-and-slab prior, see (Banerjee et al., 2021) for a recent survey. However, exact posterior computation involves summing over 2^p models, where p is the number of covariates, which is intractable for even moderate p . Markov chain Monte

Carlo (MCMC) methods avoid this problem, but are known to have difficulty efficiently exploring the model space for high-dimensional covariates (Ormerod et al., 2017), especially for the problem sizes found in many modern omics studies which motivate our work. This high computational cost has led to several methods either making continuous relaxations, giving rise to *continuous shrinkage priors* (O’Hara and Sillanpää, 2009; Banerjee et al., 2021), or computing only *maximum a posteriori* (MAP) estimates, thereby not offering the full Bayesian machinery. Since we wish to preserve certain interpretable features arising from the original discrete model selection approach, such as inclusion probabilities of particular covariates for variable selection, we instead turn to variational inference.

Variational inference (VI) is a popular scalable approximation technique, which has proven to be an effective tool for approximate Bayesian inference in many settings. VI involves minimizing the Kullback-Leibler divergence between a family of tractable distributions, called the *variational family*, and the posterior distribution; thereby recasting conditional inference as an optimization problem. The resulting minimizer is then used for downstream Bayesian inference. Though the approximation does not provide exact Bayesian inference, computationally convenient variational families can dramatically increase scalability. A common choice being *mean-field families*, under which the model parameters are independent. For a detailed review of VI, we direct the reader to Blei et al. (2017) and Zhang et al. (2019).

We propose a scalable and interpretable Bayesian proportional hazards model using a sparsity-inducing spike-and-slab prior with Laplace slab and Dirac spike, referred to as *sparse variational Bayes* (**SVB**). Since the posterior is computationally intractable, we use a mean-field variational approximation based on a factorizable family of spike-and-slab distributions, thereby preserving certain desirable discrete model selection aspects while providing scalable approximate Bayesian inference. We derive a coordinate-ascent algorithm for our implementation and investigate its performance in extensive simulations, comparing it against the posterior obtained via MCMC and demonstrating that the variational Bayes posterior can be used as a viable alternative, whilst being orders of magnitude faster to compute. We further compare with other state-of-the-art Bayesian variable selection methods, demonstrating comparable or better performance in many settings. Finally, we analyze two transcriptomic datasets involving ovarian and breast cancer data with censored survival outcomes, yielding biologically interpretable results.

Various versions of this sparse variational family have been employed in linear and logistic re-

gression models (Logsdon et al., 2010; Titsias and Lázaro-Gredilla, 2011; Carbonetto and Stephens, 2012; Ormerod et al., 2017; Ray et al., 2020; Ray and Szabó, 2021) with some of these works specifically motivated by high-dimensional genomic applications. While most of these works use Gaussian distributions for the slab component, we instead follow Ray and Szabó (2021) in using a Laplace prior slab since Gaussian prior slabs are known to cause excessive shrinkage leading to potentially poor performance, even when exact posterior computation is possible (Castillo and van der Vaart, 2012). Our work can thus be viewed as extending ideas from the sparse VI literature to the setting of survival analysis under censoring.

More generally, (not necessarily sparse) VI has proven to be an effective tool for approximate Bayesian inference and has seen wide use in several settings, including linear and logistic regression (Jaakkola and Jordan, 1996; Knowles and Minka, 2011), group factor analysis (Klami et al., 2015), topic modelling (Blei and Lafferty, 2007), clustering (Teschendorff et al., 2005) and Gaussian processes (Opper and Arachambeau, 2009) amongst others, with many of these methods employed in genomic and transcriptomic studies (Logsdon et al., 2010; Papastamoulis et al., 2014; Zhang and Flaherty, 2017; Svensson et al., 2020).

2 Materials and Methods

Notation: Let $\mathcal{D} = \{(t_i, \delta_i, x_i)\}_{i=1}^n$ denote the observed data, where $t_i \in \mathbb{R}^+$ is an observed (possibly right censored) survival time, $\delta_i \in \{0, 1\}$ is a censoring indicator with $\delta_i = 0$ if the observation is right censored and $\delta_i = 1$ if the observation is uncensored, and $x_i = (x_{i1}, \dots, x_{ip})^\top \in \mathbb{R}^p$ is a vector of explanatory variables.

2.1 Survival Analysis and the proportional hazards model

Let \mathbf{T} denote a random variable for an event time with density $f(t)$ and cumulative distribution function $F(t)$. Then the *survival function*, the probability a subject survives past time t , is given by

$$S(t) = 1 - F(t) = \exp\left(-\int_0^t h(s)ds\right) = \exp(-H(t)), \quad (1)$$

where $H(t) = \int_0^t h(s)ds$ is the cumulative hazard rate and $h(t) = f(t)/S(t)$ is the *hazard rate*, the instantaneous rate of failure at time t . Importantly, expressing $S(t)$ in terms of the hazard function

h provides a natural mechanism for analysing survival times by assuming a form for h (Ibrahim et al., 2001; Clark et al., 2003).

One such form, used to quantify the effect of features collected alongside survival times, is the *proportional hazards model* (PHM), wherein,

$$h(t; x, \beta) = h_0(t) \exp(\beta^\top x), \quad (2)$$

where $h_0(t)$ is a baseline hazard rate and $\beta = (\beta_1, \dots, \beta_p)^\top \in \mathbb{R}^p$ are the model coefficients corresponding to the potential covariates of interest. Typically, estimating β is done by maximizing the *partial likelihood*,

$$L_p(\mathcal{D}; \beta) = \prod_{\{i: \delta_i=1\}} \frac{\exp(\beta^\top x_i)}{\sum_{r \in R(t_i)} \exp(\beta^\top x_r)}, \quad (3)$$

where $R(t_i) = \{r : t_r \geq t_i\}$ (Cox, 1972, 1975). Under the partial likelihood, the baseline hazard rate $h_0(t)$ is treated as a nuisance parameter and not specified, meaning the survival function is not directly accessible without further assumptions on the hazard rate. This approach is commonly used when the main interest is on quantifying the effect of covariates on the survival time to understand the underlying mechanisms, rather than purely for predictive purposes. Since our focus is on variable selection and analysing effect sizes, we use the partial likelihood to compute the posterior.

The use of the partial likelihood (3) is common in Bayesian survival analysis, and can be understood via multiple Bayesian and frequentist justifications (Ibrahim et al., 2001). For the frequentist, the partial likelihood is the empirical likelihood with the maximum likelihood estimator (MLE) for the cumulative baseline hazard function H_0 plugged in, i.e. the profile likelihood (Murphy and Van Der Vaart, 2000). Using it in a Bayesian way thus means we are fitting a prior to our parameter of interest β and an MLE on the nuisance parameter H_0 . For the Bayesian, assigning a Gamma process prior to H_0 , marginalizing the posterior over H_0 and taking the limit as the prior on H_0 becomes non-informative, gives a marginal posterior for β exactly based on the partial likelihood (3) (Kalbfleisch, 1978). Thus using (3) can be viewed as using a diffuse Gamma process prior on the nuisance parameter H_0 .

2.2 Prior and variational family

We consider a spike-and-slab prior (George and McCulloch, 1993; Mitchell and Beauchamp, 1988) for the model coefficients β . Our choice of prior is conceptually natural for variable selection problems as it leads to interpretable inference regarding the inclusion probabilities of individual features. However, unlike the original formulation which uses Gaussian slabs, we use Laplace slabs, since Gaussian slabs are known to overly shrink the true large signals (Castillo and van der Vaart, 2012; Ray and Szabó, 2021). Formally, the prior distribution, $\Pi(\beta, z, w)$, has hierarchical representation,

$$\begin{aligned} \beta_j | z_j &\stackrel{\text{ind}}{\sim} z_j \text{Laplace}(\lambda) + (1 - z_j) \delta_0 \\ z_j | w_j &\stackrel{\text{ind}}{\sim} \text{Bernoulli}(w_j) \\ w_j &\stackrel{\text{iid}}{\sim} \text{Beta}(a_0, b_0), \end{aligned} \tag{4}$$

where δ_0 is a Dirac mass at zero, $\text{Laplace}(\lambda)$ has density function $\frac{\lambda}{2} e^{-\lambda|x|}$ on \mathbb{R} and $\lambda, a_0, b_0 > 0$. Placing a hyperprior on (w_j) allows mixing over the sparsity level and allows adaptation to the unknown sparsity. The posterior density is proportional to the partial likelihood L_p in (3) times the joint prior density, formally,

$$\pi(\beta, z, w | \mathcal{D}) \propto L_p(\mathcal{D}; \beta) \pi(\beta, z, w), \tag{5}$$

where $\beta = (\beta_1, \dots, \beta_p)^\top \in \mathbb{R}^p$, $z = (z_1, \dots, z_p)^\top \in \{0, 1\}^p$ and $w = (w_1, \dots, w_p)^\top \in [0, 1]^p$.

Since the posterior (5) is computationally intractable, we use a variational approximation. For the variational family, we choose a mean-field family given by the product of independent spike-and-slab distributions with normal slab and Dirac spike for each coefficient:

$$\mathcal{Q} = \left\{ Q_{\mu, \sigma, \gamma} = \bigotimes_{j=1}^p [\gamma_j N(\mu_j, \sigma_j^2) + (1 - \gamma_j) \delta_0] \right\}, \tag{6}$$

where $\mu_j \in \mathbb{R}$, $\sigma_j \in \mathbb{R}^+$, $\gamma_j \in [0, 1]$. The notation \otimes means a product measure implying coordinate independence, so that $\beta \sim Q_{\mu, \sigma, \gamma}$ means

$$\beta_j \stackrel{\text{ind}}{\sim} \gamma_j N(\mu_j, \sigma_j^2) + (1 - \gamma_j) \delta_0.$$

Our choice of \mathcal{Q} thereby provides scalability and maintains the property of variable selection via

the Dirac mass, since the quantities $\gamma_j = Q(\beta_j \neq 0)$ are the inclusion probabilities. The variational posterior is then given by finding an element $Q \in \mathcal{Q}$ minimizing the KL divergence between Q and the posterior distribution $\Pi(\cdot|\mathcal{D})$,

$$\tilde{\Pi} = \underset{Q_{\mu, \sigma, \gamma} \in \mathcal{Q}}{\operatorname{argmin}} \operatorname{KL}(Q_{\mu, \sigma, \gamma} \parallel \Pi(\cdot|\mathcal{D})), \quad (7)$$

which is then used for inference. Note this approximation has $O(p)$ parameters compared to the full posterior dimension $O(2^p)$. As with all mean-field approximation, dependent information between the components of β are lost, such as whether two coefficients β_i and β_j are likely to be selected simultaneously or not.

2.3 Coordinate-ascent algorithm

A convenient method for computing the mean-field variational posterior $\tilde{\Pi}$ is coordinate-ascent variational inference (CAVI) (Blei et al., 2017). In CAVI, the parameters $\mu_j, \sigma_j, \gamma_j$ for $j = 1, \dots, p$ are sequentially updated by finding the values that minimize the KL divergence between the variational family and the posterior, whilst all other parameters are kept fixed, iterating until convergence. This reduces the overall optimization problem to a sequence of one-dimensional optimization problems.

Minimizing the objective (7) is intractable for the Bayesian PHM due to the form of likelihood (3) and so we instead minimize an upper bound for the KL divergence. Such surrogate type functionals are well-used in variational inference, for example in logistic regression (Jaakkola and Jordan, 1996; Knowles and Minka, 2011; Depraetere and Vandebroek, 2017), and can lead to an increase in accuracy.

The component-wise variational updates for μ_j and σ_j are given by the minimizers of

$$f(\mu_j; \mu_{-j}, \sigma, \gamma, z_j = 1) = \sum_{\{i: \delta_i = 1\}} \left(\log \sum_{r \in R(t_i)} M(x_{rj}, \mu_j, \sigma_j) P_j(x_r, \mu, \sigma, \gamma) - \mu_j x_{ij} \right) + \lambda \sigma_j \sqrt{2/\pi} e^{-\mu_j^2/(2\sigma_j^2)} + \lambda \mu_j (1 - 2\Phi(-\mu_j/\sigma_j)) \quad (8)$$

and

$$g(\sigma_j; \mu, \sigma_{-j}, \gamma, z_j = 1) = \sum_{\{i:\delta_i=1\}} \left(\log \sum_{r \in R(t_i)} M(x_{rj}, \mu_j, \sigma_j) P_j(x_r, \mu, \sigma, \gamma) \right) + \lambda \sigma_j \sqrt{2/\pi} e^{-\mu_j^2/(2\sigma_j^2)} + \lambda \mu_j (1 - 2\Phi(-\mu_j/\sigma_j)) - \log \sigma_j \quad (9)$$

where $M(x_{rj}, \mu_j, \sigma_j) = \exp(\mu_j x_{rj} + \frac{1}{2} \sigma_j^2 x_{rj}^2)$, $P_j(x_r, \mu, \sigma, \gamma) = \prod_{k \neq j} (\gamma_k M(x_{rk}, \mu_k, \sigma_k) + (1 - \gamma_k))$ and Φ denotes the CDF of the standard normal distribution. The minimizers of these expressions do not have closed-form solutions, and therefore optimization routines are needed to find them, for instance via Brent's method (Brent, 1973). Finally, the component-wise variational update for γ_j is given by solving,

$$\log \frac{\gamma_j}{1 - \gamma_j} = \frac{1}{2} + \log \frac{a_0}{b_0} - \left(\lambda \sigma_j \sqrt{2/\pi} e^{-\frac{\mu_j^2}{2\sigma_j^2}} + \lambda \mu_j (1 - 2\Phi(-\frac{\mu_j}{\sigma_j})) + \log \frac{\sqrt{2}}{\sqrt{\pi} \sigma_j \lambda} \right) + \sum_{\{i:\delta_i=1\}} \left(\log \sum_{r \in R(t_i)} M(x_{rj}, \mu_j, \sigma_j) P_j(x_r, \mu, \sigma, \gamma) - \log \sum_{r \in R(t_i)} P_j(x_r, \mu, \sigma, \gamma) - \mu_j x_{ij} \right) \quad (10)$$

A full derivation of these expressions is provided in Section A of the Supplement.

Algorithm 1 summarizes the coordinate-ascent variational inference algorithm. We denote the RHS of (10) by $\zeta(\gamma_j; \mu, \sigma, \gamma_{-j})$, and assess convergence by computing the change in μ, σ and γ after each iteration, stopping when the total absolute change is below a specified threshold (e.g. 10^{-3}). While the evidence lower bound (ELBO) is often used to assess convergence, the ELBO is not analytically tractable in the present setting, which instead requires computationally expensive Monte Carlo integration to evaluate it. For this reason, we instead choose to assess convergence using the absolute change in μ, σ and γ .

Due to the non-convex objective in (7), CAVI generally only guarantees convergence to a local optimum, and therefore can be sensitive to initialization (Blei et al., 2017). We found this to be the case for our method, particularly for μ and γ , therefore providing good starting values is generally important (see Section D of the Supplementary materials for more details). In turn, we initialized μ using the LASSO with a small regularization hyperparameter, since μ corresponds to the unshrunk means if the variables are included in the model, and γ as $(0.5, \dots, 0.5)^\top$, since this corresponds to an initial inclusion probability of 0.5 for each feature. We found the proposed method is less sensitive to initial value of σ , for example initializing σ as $(0.05, \dots, 0.05)^\top$ is sufficient.

Algorithm 1 CAVI for VB approximation to posterior (5)

```
1: require  $\mathcal{D}, \lambda, a_0, b_0$ 
2: Initialize  $\mu, \sigma, \gamma$ 
3: while not converged
4:   for  $j = 1, \dots, p$ 
5:      $\mu_j \leftarrow \operatorname{argmin}_{\mu_j \in \mathbb{R}} f(\mu_j; \mu_{-j}, \sigma, \gamma, z_j = 1)$  // Equation (8)
6:      $\sigma_j \leftarrow \operatorname{argmin}_{\sigma_j \in \mathbb{R}^+} g(\sigma_j; \mu, \sigma_{-j}, \gamma, z_j = 1)$  // Equation (9)
7:      $\gamma_j \leftarrow \operatorname{sigmoid} \zeta(\gamma_j; \mu, \sigma, \gamma_{-j})$  // Equation (10)
8: return  $\mu, \sigma, \gamma$ .
```

2.4 Parameter tuning

The proposed method involves three prior parameters λ, a_0 and b_0 defined in (4), where λ controls the shrinkage imposed on $\beta_j | z_j = 1$, with large values imposing more shrinkage, and a_0 and b_0 control the shape of the Beta distribution, whose expectation $a_0 / (a_0 + b_0)$ reflects the *a priori* proportion of non-zero coefficients. Generally, our method is not particularly sensitive to the prior parameters (see Section D of the Supplement for a numerical investigation) and in practice using sensible *a priori* choices is appropriate for most settings. For example, if it is believed there are a small number of non-zero coefficients with moderate effect sizes, taking a_0 as a small constant (such as 1, 10, $p/100$), $b_0 = p$ and λ between 0.5 and 2.0 is appropriate.

If an *a priori* choice is unavailable, the prior parameters can be tuned using the data. To do so, we suggest performing a grid search over a predefined set of values, selecting the element that maximizes a given goodness of fit measure, several options of which are presented in section B of the Supplement. Furthermore, when tuning a_0 and b_0 , to limit computation we suggest fixing b_0 and searching across a set of values for a_0 , thereby exploring different values of the *a priori* inclusion probability.

2.5 Implementation

A freely available implementation is available for the R programming language via the package `survival.svb`, with functions available for fitting and evaluating models.

Setting	c	Method	ℓ_2 -error	ℓ_1 -error	TPR	FDR	AUC	runtime
1	0.25	SVB	0.368 (0.21, 0.70)	1.000 (0.52, 1.86)	1.000 (0.90, 1.00)	0.000 (0.00, 0.00)	1.000 (1.00, 1.00)	18.5s (13.5s,25.6s)
		MCMC	0.412 (0.20, 0.75)	1.017 (0.48, 2.01)	1.000 (0.90, 1.00)	0.000 (0.00, 0.00)	1.000 (1.00, 1.00)	1h 24m (1h 7m,1h 50m)
	0.4	SVB	0.428 (0.23, 0.89)	1.138 (0.63, 2.45)	1.000 (0.90, 1.00)	0.000 (0.00, 0.00)	1.000 (0.95, 1.00)	21.9s (14.5s,30.5s)
		MCMC	0.506 (0.26, 0.98)	1.300 (0.69, 2.74)	1.000 (0.80, 1.00)	0.000 (0.00, 0.00)	1.000 (1.00, 1.00)	1h 28m (1h 25m,1h 30m)
2	0.25	SVB	0.376 (0.20, 0.73)	1.031 (0.58, 2.07)	1.000 (0.90, 1.00)	0.000 (0.00, 0.00)	1.000 (1.00, 1.00)	18.9s (14.4s,25.4s)
		MCMC	0.405 (0.21, 0.81)	1.059 (0.58, 2.18)	1.000 (0.90, 1.00)	0.000 (0.00, 0.00)	1.000 (1.00, 1.00)	1h 14m (1h 6m,1h 17m)
	0.4	SVB	0.472 (0.23, 1.08)	1.176 (0.61, 2.96)	1.000 (0.90, 1.00)	0.000 (0.00, 0.00)	1.000 (0.95, 1.00)	24.0s (17.3s,33.1s)
		MCMC	0.520 (0.25, 1.08)	1.319 (0.62, 2.91)	1.000 (0.90, 1.00)	0.000 (0.00, 0.00)	1.000 (1.00, 1.00)	1h 38m (1h 25m,2h 4m)
3	0.25	SVB	0.392 (0.18, 1.40)	1.079 (0.53, 3.28)	1.000 (0.90, 1.00)	0.000 (0.00, 0.09)	1.000 (0.95, 1.00)	29.2s (16.9s,44.9s)
		MCMC	0.418 (0.21, 1.01)	1.092 (0.54, 2.58)	1.000 (0.90, 1.00)	0.000 (0.00, 0.00)	1.000 (1.00, 1.00)	1h 45m (1h 24m,1h 49m)
	0.4	SVB	0.470 (0.24, 1.57)	1.263 (0.63, 4.16)	1.000 (0.80, 1.00)	0.000 (0.00, 0.10)	1.000 (0.95, 1.00)	21.7s (13.7s,33.2s)
		MCMC	0.508 (0.23, 1.26)	1.236 (0.61, 3.45)	1.000 (0.80, 1.00)	0.000 (0.00, 0.09)	1.000 (1.00, 1.00)	1h 36m (1h 30m,1h 45m)
4	0.25	SVB	0.393 (0.18, 1.12)	1.067 (0.50, 2.54)	1.000 (0.90, 1.00)	0.000 (0.00, 0.10)	1.000 (0.95, 1.00)	17.0s (9.2s,24.9s)
		MCMC	0.382 (0.17, 0.95)	1.007 (0.44, 2.47)	1.000 (0.90, 1.00)	0.000 (0.00, 0.10)	1.000 (1.00, 1.00)	1h 5m (1h 3m,1h 8m)
	0.4	SVB	0.425 (0.18, 1.38)	1.171 (0.50, 2.85)	1.000 (0.90, 1.00)	0.000 (0.00, 0.10)	1.000 (0.95, 1.00)	25.8s (14.8s,39.9s)
		MCMC	0.486 (0.21, 1.13)	1.158 (0.53, 3.17)	1.000 (0.80, 1.00)	0.000 (0.00, 0.00)	1.000 (0.95, 1.00)	1h 38m (1h 14m,1h 46m)

Table 1: Comparison of variational to MCMC posterior taking $(n, p, s) = (200, 1000, 10)$ and $c \in \{0.25, 0.4\}$, presented is the median and (5%, 95%) quantiles. Simulations were ran on Intel[®] Xeon[®] E5-2680 v4 2.40GHz CPUs.

3 Simulation study

We use simulations to validate the proposed method, referred to as **SVB**. Firstly, we compare the variational posterior to the posterior obtained via Markov-Chain Monte-Carlo (MCMC), assessing whether our approximation can be used as a viable alternative. Secondly, we compare against other state-of-the-art Bayesian variable selection methods for the proportional hazards model. R scripts to reproduce our results can be found at <https://github.com/mkomod/svb.exp>

3.1 Simulation design

Data is simulated for $i = 1, \dots, n$ observations, each having a survival time t_i , censoring indicator δ_i , and p continuous predictors $x_i \in \mathbb{R}^p$. The survival time is sampled independently from $\mathbf{T} \mid x_i, \beta_0, h_0$, which has density $f(t; x, \beta_0, h_0) = h_0(t) \exp\left(\beta_0^\top x - e^{\beta_0^\top x} \int_0^t h_0(s) ds\right)$, where we have taken $h_0(t) = 1$ and where the coefficient vector $\beta_0 \in \mathbb{R}^p$ contains s non-zero elements with values sampled iid. uniformly from $[-2.0, -0.5] \cup [0.5, 2.0]$ and indices chosen uniformly at random. To introduce censoring, we sample $d_i \stackrel{\text{iid}}{\sim} U(0, 1)$, letting $\delta_i = \mathbb{I}(d_i > c)$ where $c \in [0, 1]$ is the censoring proportion, and set $t_i \leftarrow t'_i$ where $t'_i \stackrel{\text{ind}}{\sim} U(0, t_i)$ if $\delta_i = 0$, leaving t_i unchanged otherwise. Finally, the predictors

are generated from one of four different settings designed to examine the behaviour under varying degrees of difficulty:

- *Setting 1*, an independent setting where $x_i \stackrel{\text{iid}}{\sim} N(0_p, I_p)$.
- *Setting 2*, a fairly challenging setting where predictors are moderately correlated within groups and independent between groups, formally $x_i \stackrel{\text{iid}}{\sim} N(0, \Sigma)$ with $\text{diag}(\Sigma) = 1$, $\Sigma_{ij} = 0.6$ for $i \neq j$, $i, j = 50k + 1, \dots, 50(k + 1)$, $k = 0, \dots, p/50 - 1$, $\Sigma_{ij} = 0$ otherwise. The setting is similar to [Tang et al. \(2017\)](#).
- *Setting 3*, a challenging setting where $x_i \stackrel{\text{iid}}{\sim} N(\mu, \Sigma)$ with μ, Σ estimated from the design of the TCGA dataset analyzed in [Section 4.1](#). The s causal variables are randomly selected to correspond to features with a variance of at least 1.0.
- *Setting 4*, a realistic setting where the first p predictors are taken from the TCGA dataset analyzed in [Section 4.1](#) and the s causal features are selected as in [setting 3](#).

To evaluate the methods, we examine the accuracy of the corresponding point estimates, quality of the variables selected, and (if applicable) the uncertainty quantification. The point estimates are assessed via the ℓ_2 -error, $\|\beta_0 - \hat{\beta}\|$ and the ℓ_1 -error, $|\beta_0 - \hat{\beta}|$, where $\hat{\beta}$ is either a MAP estimate for β or the posterior mean if a distribution is available. For the variables selected the: (i) true positive rate (TPR) (ii) false discovery rate (FDR) and (iii) area under the curve (AUC) of the receiver operator characteristic curve are computed. For the TPR and FDR a coefficient is considered to have been selected if the posterior inclusion probability is at least 0.5. Finally, regarding uncertainty quantification, we evaluate the marginal credible sets by computing the: (i) empirical coverage, i.e. the proportion of times the true coefficient $\beta_{0,j}$ is contained in the credible set, and (ii) set size, given by the Lebesgue measure of the set. Details regarding the construction of the credible sets are presented where appropriate. For all metrics, we report the median, 5% and 95% quantiles across 100 replicates unless otherwise stated.

3.2 Simulation results

3.2.1 Comparison to MCMC

To assess how well the variational posterior matches the target (computationally challenging) posterior from [\(5\)](#), we compare the performance of our approach against the approximate yet asymptot-

ically exact posterior obtained via MCMC. To do so, data is generated as described in Section 3.1, taking $(n, p, s) = (200, 1000, 10)$ and $c \in \{0.25, 0.4\}$, where we have kept n and p small so we can run our MCMC sampler in a reasonable amount of time. The MCMC sampler (described in Section C.1 of the Supplement) was run for 10,000 iterations with a burn-in period of 1,000 iterations. For both methods we used prior parameters $\lambda = 1, a_0 = 1$ and $b_0 = p$. Results are presented in Table 1.

Regarding the point estimates, for both the MCMC and the variational posteriors we took $\hat{\beta} = (\hat{\beta}_1, \dots, \hat{\beta}_p) \in \mathbb{R}^p$ as the posterior mean, which for the latter is given by $\hat{\beta}_j = \gamma_j \mu_j$. Promisingly, both methods produce similar results, with near identical performance in all settings (Table 1). In particular, the similarity of the ℓ_2 -error and ℓ_1 -error suggests the posterior means are near identical. In terms of variable selection, both methods performed similarly. In particular, the TPR is comparable across the different settings, suggesting both methods are selecting a similar set of truly associated features. However, the upper quantile for the FDR is slightly larger for the variational posterior, meaning the MCMC posterior selects fewer spurious variables.

Finally, we examine the uncertainty quantification of each method via 95% marginal credible sets $S_j, j = 1, \dots, p$, which are given by: $S_j = I_j$ if the posterior inclusion probability is greater than 0.95, $S_j = \{0\}$ if the posterior inclusion probability is less than 0.05, and $S_j = I_j \cup \{0\}$ otherwise, where I_j is the smallest interval from the continuous component of our posterior such that S_j contains 95% of the posterior mass. As expected, for the non-zero coefficients, the coverage of the MCMC posterior is slightly better than the coverage of the variational posterior (Table 2), meaning the credible sets of the variational posterior are sometimes not large enough to capture the true non-zero coefficients. This is further reflected by the smaller set sizes, highlighting the well known fact that VI can underestimate the posterior variance (Carbonetto and Stephens, 2012; Blei et al., 2017; Zhang et al., 2019; Ray et al., 2020). Promisingly, the coverage of the zero coefficients is equal to one for both methods, meaning the credible sets contain zero, and typically, as reflected by the set size, contain only zero.

Overall, the variational posterior displays similar performance to the MCMC posterior in key aspects for this setting with $p = 1000$, and can be computed orders of magnitude faster (Table 1). Our results highlight that the variational posterior is particularly good at capturing the key features (posterior means and inclusion probabilities) and provides reasonable uncertainty quantification for individual features.

Setting	c	Method	cov. $\beta_0 \neq 0$	set size $\beta_0 \neq 0$	cov. $\beta_0 = 0$	set size $\beta_0 = 0$
1	0.25	SVB	0.770 (0.202)	0.320 (0.013)	1.000 (0.000)	0.000 (0.000)
		MCMC	0.928 (0.138)	0.506 (0.039)	1.000 (0.000)	0.000 (0.000)
	0.4	SVB	0.774 (0.208)	0.355 (0.021)	1.000 (0.000)	0.000 (0.000)
		MCMC	0.914 (0.127)	0.570 (0.054)	1.000 (0.000)	0.000 (0.000)
2	0.25	SVB	0.703 (0.227)	0.306 (0.028)	1.000 (0.001)	0.000 (0.000)
		MCMC	0.904 (0.161)	0.522 (0.053)	1.000 (0.000)	0.000 (0.000)
	0.4	SVB	0.683 (0.262)	0.333 (0.039)	1.000 (0.001)	0.000 (0.000)
		MCMC	0.845 (0.218)	0.567 (0.101)	1.000 (0.000)	0.000 (0.000)
3	0.25	SVB	0.626 (0.288)	0.251 (0.020)	1.000 (0.000)	0.000 (0.000)
		MCMC	0.903 (0.140)	0.482 (0.047)	1.000 (0.000)	0.000 (0.000)
	0.4	SVB	0.619 (0.278)	0.276 (0.028)	1.000 (0.000)	0.000 (0.000)
		MCMC	0.873 (0.197)	0.540 (0.078)	1.000 (0.000)	0.000 (0.000)
4	0.25	SVB	0.672 (0.224)	0.252 (0.021)	1.000 (0.000)	0.000 (0.000)
		MCMC	0.921 (0.144)	0.483 (0.047)	1.000 (0.000)	0.000 (0.000)
	0.4	SVB	0.660 (0.249)	0.277 (0.025)	1.000 (0.001)	0.000 (0.000)
		MCMC	0.906 (0.156)	0.547 (0.059)	1.000 (0.000)	0.000 (0.000)

Table 2: Coverage and set size for variational and MCMC posterior. Presented are means and std. dev.

3.2.2 Comparison to other methods

We perform a large-scale simulation study to empirically compare the performance of our method to two Bayesian variable selection methods. Within our study, data is generated as described in Section 3.1, taking $(n, p, s) = (500, 5000, 30)$ and $c \in \{0.25, 0.4\}$ for all settings. Notably, under such a setting running MCMC would be computationally prohibitive, as highlighted in the previous section.

We compare against **BhGLM** (Tang et al., 2017), a spike-and-slab LASSO method that uses a mixture of Laplace distributions with one acting as the spike and the other the slab, and **BVSNLP** (Nikooienejad et al., 2020), which uses a mixture prior composed of a point mass at zero and an inverse moment prior. Notably, both **BhGLM** and **BVSNLP** use Cox’s partial likelihood in the posterior and return a MAP estimate for β as well as posterior inclusion probabilities for each feature. Finally, for each method we use the default hyperparameters and let $\lambda = 1$, $a_0 = 1$ and $b_0 = p$ for **SVB**.

Generally, all methods produced excellent point estimates, with **SVB** obtaining the smallest

median ℓ_2 -error and ℓ_1 -error in settings 1 and 2, and **BhGLM** in setting 4 (Table 3). Notably, **SVB** obtained the smallest lower (5%) quantile for the ℓ_2 -error and ℓ_1 -error in settings 3 and 4, meaning the method can perform better than **BhGLM** but may be sensitive to the design matrix.

Regarding the variables selected, all methods performed exceptionally well achieving the ideal values for the TPR, FDR and AUC in Settings 1 and 2 (Table 3). Within settings 3, **BhGLM** obtained the best TPR, FDR and AUC closely followed by **SVB** and **BVSNLP**. Within setting 4, all three methods obtained the ideal values when the censoring was low ($c = 0.25$) and **BhGLM** performed best under moderate censoring ($c = 0.40$). Further, **BhGLM** best controlled the FDR in settings 3 and 4, obtaining the lowest upper (95%) quantile, closely followed by **SVB**. Finally, we note, **SVB** is the only method that provides uncertainty quantification, a direct application of which is demonstrated in Section 4.2.

4 Application

4.1 TCGA ovarian cancer data

The first dataset we analyzed is a transcriptomic dataset where the outcome of interest is overall survival. The dataset was collected from patients with ovarian cancer and has a sample size of $n = 580$, of which 229 samples are right censored and 351 samples are uncensored, corresponding to a censoring rate of 39.5% (TCGA, 2022). Within the dataset there are $p = 12,042$ covariates, which we pre-processed by removing features with a coefficient of variation below the median value (Mar et al., 2011), leaving 6,021 covariates which we centered before fitting our method.

When applying our method, we set $a_0 = p/100$ and $b_0 = p$, reflecting our prior belief that few genes are associated with the response. As we had no prior belief for λ , we performed 10-fold cross validation to select the value, exploring a grid of values $\Lambda = \{0.05, 0.1, 0.25, 0.5, 0.75, 1.0, 1.25, 1.5, 1.75, 2.0, 2.5, 3.0, 4.0, 5.0\}$. To evaluate model fit we compute the: (i) ELBO = $\mathbb{E}_Q[\log L_p] - \text{KL}(Q||\Pi)$, (ii) expected log-likelihood under the variational posterior (ELL = $\mathbb{E}_Q[\log L_p(\mathcal{D}; \beta)]$), and (iii) c-index, reporting the mean and standard deviation across the 10 folds for the training and validation sets in Table 7 of the Supplement. Notably, no single hyperparameter value stands out as being best, meaning the model is not particularly sensitive to the value of λ .

To assess the model’s convergence diagnostics we examine the fit for $\lambda = 1$, and examine the

Setting	c	Method	ℓ_2 -error	ℓ_1 -error	TPR	FDR	AUC
1	0.25	SVB	0.378 (0.26, 0.89)	1.747 (1.16, 4.17)	1.000 (1.00, 1.00)	0.000 (0.00, 0.00)	1.000 (1.00, 1.00)
		BhGLM	1.206 (0.79, 1.78)	9.590 (7.22, 12.88)	1.000 (1.00, 1.00)	0.000 (0.00, 0.00)	1.000 (1.00, 1.00)
		BVSNLP	0.456 (0.33, 0.96)	2.007 (1.41, 4.57)	1.000 (1.00, 1.00)	0.000 (0.00, 0.03)	1.000 (1.00, 1.00)
	0.4	SVB	0.449 (0.31, 0.99)	2.056 (1.37, 4.87)	1.000 (1.00, 1.00)	0.000 (0.00, 0.00)	1.000 (1.00, 1.00)
		BhGLM	0.807 (0.53, 1.35)	6.458 (4.52, 9.31)	1.000 (1.00, 1.00)	0.000 (0.00, 0.00)	1.000 (1.00, 1.00)
		BVSNLP	0.518 (0.35, 1.44)	2.231 (1.52, 6.85)	1.000 (0.96, 1.00)	0.000 (0.00, 0.03)	1.000 (0.99, 1.00)
2	0.25	SVB	0.405 (0.29, 0.80)	1.823 (1.28, 3.78)	1.000 (1.00, 1.00)	0.000 (0.00, 0.00)	1.000 (1.00, 1.00)
		BhGLM	0.596 (0.45, 1.04)	4.494 (3.51, 6.89)	1.000 (1.00, 1.00)	0.000 (0.00, 0.00)	1.000 (1.00, 1.00)
		BVSNLP	0.475 (0.33, 0.90)	2.130 (1.47, 4.01)	1.000 (1.00, 1.00)	0.000 (0.00, 0.00)	1.000 (1.00, 1.00)
	0.4	SVB	0.491 (0.33, 1.05)	2.208 (1.45, 5.03)	1.000 (0.97, 1.00)	0.000 (0.00, 0.03)	1.000 (1.00, 1.00)
		BhGLM	0.551 (0.44, 0.86)	3.716 (2.98, 5.36)	1.000 (0.97, 1.00)	0.000 (0.00, 0.00)	1.000 (1.00, 1.00)
		BVSNLP	0.515 (0.37, 1.47)	2.238 (1.54, 6.71)	1.000 (1.00, 1.00)	0.000 (0.00, 0.00)	1.000 (1.00, 1.00)
3	0.25	SVB	1.040 (0.30, 3.17)	3.881 (1.36, 15.37)	0.967 (0.83, 1.00)	0.000 (0.00, 0.14)	0.983 (0.92, 1.00)
		BhGLM	0.590 (0.36, 1.57)	3.279 (2.23, 6.73)	1.000 (0.93, 1.00)	0.000 (0.00, 0.03)	1.000 (0.97, 1.00)
		BVSNLP	3.107 (1.74, 9.73)	12.262 (6.88, 47.67)	0.967 (0.53, 1.00)	0.000 (0.00, 0.53)	0.983 (0.78, 1.00)
	0.4	SVB	1.379 (0.36, 3.47)	5.728 (1.55, 17.47)	0.933 (0.77, 1.00)	0.033 (0.00, 0.13)	0.967 (0.88, 1.00)
		BhGLM	0.796 (0.41, 2.18)	4.035 (2.25, 10.92)	0.967 (0.87, 1.00)	0.000 (0.00, 0.07)	1.000 (0.95, 1.00)
		BVSNLP	3.867 (1.98, 11.44)	15.874 (7.99, 51.07)	0.967 (0.20, 1.00)	0.033 (0.00, 0.69)	0.983 (0.65, 1.00)
4	0.25	SVB	0.603 (0.29, 2.02)	2.298 (1.21, 8.84)	1.000 (0.90, 1.00)	0.000 (0.00, 0.08)	1.000 (0.95, 1.00)
		BhGLM	0.503 (0.35, 1.36)	3.141 (2.25, 5.59)	1.000 (0.93, 1.00)	0.000 (0.00, 0.03)	1.000 (0.97, 1.00)
		BVSNLP	2.946 (1.96, 8.72)	11.426 (6.98, 36.46)	1.000 (0.90, 1.00)	0.000 (0.00, 0.07)	1.000 (0.95, 1.00)
	0.4	SVB	1.092 (0.32, 2.83)	3.878 (1.40, 14.06)	0.967 (0.83, 1.00)	0.000 (0.00, 0.08)	0.983 (0.92, 1.00)
		BhGLM	0.674 (0.40, 1.64)	3.610 (2.28, 7.72)	1.000 (0.93, 1.00)	0.000 (0.00, 0.04)	1.000 (0.97, 1.00)
		BVSNLP	3.163 (2.14, 10.53)	12.227 (8.14, 45.64)	1.000 (0.73, 1.00)	0.000 (0.00, 0.32)	1.000 (0.87, 1.00)

Table 3: Comparison of Bayesian variable selection methods, taking $(n, p, s) = (500, 5000, 30)$ and $c \in \{0.25, 0.4\}$, presented is the median and (5%, 95%) quantiles.

change in: (i) ELBO, (ii) ELL, and (iii) KL between the variational posterior and the prior, as we iterate our co-ordinate ascent algorithm (Figure 1). Note the ELBO and ELL are computed for the training and validation sets, whereas $\text{KL}(Q\|\Pi)$ need only be computed for the training set. Notably, across the different folds the ELBO is increasing as the co-ordinate ascent algorithm is iterated [Figures 1 (A) and (B)], suggesting that the model fit is improving. Interestingly, the training ELL is decreasing [Figure 1 (C)], whereas the inverse is true for the validation ELL [Figure 1 (D)], meaning, initially the model is overfitting to the training data, and as we iterate begins to fit better to the unseen validation set. Further, the $\text{KL}(Q\|\Pi)$ is decreasing [Figure 1 (E)], therefore a greater degree of sparsity is enforced as we iterate, excluding more features and preserving the

ones that best explain the variation in the response.

As we are using our model for variable selection, we examine the genes selected across the different values of λ and folds. Table 4 reports the names and selection proportion of genes, where the selection proportion is the number of times a particular gene has posterior inclusion probability greater than

$$k^* = \operatorname{argmax}_{k \in [0,1]} \left\{ \frac{\sum_{j=1}^p (1 - \gamma_j) \mathbb{I}\{\gamma_j > k\}}{\sum_{j=1}^p \mathbb{I}\{\gamma_j > k\}} < \alpha \right\} \quad (11)$$

Notably, k^* is computed for each fit and is a threshold used to control the Bayesian false discovery rate at significance level α , which we have set as $\alpha = 0.10$ (Newton et al., 2004). Promisingly, the most frequently selected gene, *PI3*, has a known, albeit limited, role in ovarian cancer, a disease characterised by copy number aberration. Clauss et al. (2010) reported the first link of *PI3* gene product (elafin) to ovarian cancer (Clauss et al., 2010). Elafin, a serine proteinase inhibitor involved in inflammation and wound healing, is overexpressed in ovarian cancer and overexpression is associated with poor overall survival and is due, in part, to genomic gains on chromosome 20q13.12, a locus frequently amplified in ovarian carcinomas. There is less known about the gene encoding the alpha isoform of the calcineurin catalytic subunit (*PPP3CA*) in ovarian cancer. A recent report indicates that higher expression of calcineurin predicts poor prognosis in ovarian cancer, particularly those of serous histology (Xin et al., 2019). It is also plausible that other known functions of calcineurin/nuclear factor of activated T cells (NFAT), in controlling adaptive T-cell function or innate immunity (Fric et al., 2012), in this cancer that warrants further investigation. Finally, *CCR7*, the third most abundant gene was recently reported, in single cell RNA-seq analysis, to be emphasised in high-grade serous ovarian cancer (Izar et al., 2020).

PI3	PPP3CA	CCR7	SDF2L1	D4S234E	VSIG4	DAP	IL7R
0.7	0.379	0.293	0.286	0.229	0.171	0.136	0.136
TBP	ACSL3	SLAMF7	UBD	IL2RG	GALNT10	FLJ20323	RNF128
0.121	0.114	0.1	0.1	0.064	0.057	0.05	0.05

Table 4: Gene names and selection proportions for ovarian cancer dataset.

4.2 Breast cancer data set

The second dataset we analyzed is a transcriptomic dataset collected from patients with breast cancer, where the outcome of interest is overall survival (Yau et al., 2010). The dataset consists of $n = 682$ samples and $p = 9,168$ features which we preprocessed as before, leaving $p = 4,584$ features. Within the dataset 454 observations are right censored, corresponding to a censoring rate of 66.5%.

As in the previous section, we set $a_0 = p/100$ and $b_0 = p$, and tuned the prior parameter λ via 10-fold cross validation using the same set Λ . Table 8 in the Supplement reports the ELBO, ELL and c-index averaged across the validation and training sets. We note that the model is not particularly sensitive to the value of λ . Furthermore, an assessment of the convergence diagnostics for $\lambda = 2.5$, presented in Figure 14 of the Supplement, carries a similar interpretation as with the TCGA data.

Table 5 reports the names and selection proportions of the genes within the dataset. The most frequently selected gene, Rho GTPase activating protein 28 (*ARHGAP28*) is a negative regulator of RhoA. There is paucity of data on this gene in cancer generally, however, a report by Planche et al. (2011) identified the gene as downregulated in reactive stroma of prostate tumours. Further assessment of this gene in breast cancer is warranted. Notably, *NEK2*, *GREM1* and *ABCC5* have been examined in the biomedical literature, and have been associated with cancer cell proliferation and metastasis. More specially, overexpression of *NEK2* induces epithelial-to-mesenchymal transition, a process which leads to functional changes in cell invasion, overexpression of *GREM1* has been associated with metastasis and poor prognosis, and *ABCC5* has been associated with breast cancer skeletal metastasis (Rivera-Rivera et al., 2021; Park et al., 2020; Mourskaia et al., 2012). As with the TCGA data, it is encouraging that genes with pre-existing biological interpretation have been selected by our model.

ARHGAP28	NEK2	ABCC5	GREM1	DUSP4	ITGA5	CCL2	IGFBP7
0.386	0.25	0.2	0.2	0.193	0.193	0.164	0.143
NFE2L3	TRPC1	PKMYT1	DDX31	EMILIN1	SSPN	ABO	HSPC072
0.114	0.114	0.1	0.086	0.086	0.086	0.079	0.079

Table 5: Gene names and selection proportions for the breast cancer dataset.

Finally, we want to highlight that our method, in contrast to the methods compared in Section 3.2.2, quantifies the uncertainty of β . Crucially, the availability of uncertainty serves as a pow-

erful inferential tool for computing (variational) posterior probabilities with respect to risk scores ($\beta^\top x$). Such probabilities can be useful in comparing patients between one another, or assessing the risk of patients against chosen benchmarks (depending on the aims of the practitioner).

To demonstrate, we opt to compute the posterior probability that one patient is at greater risk than another, formally, $\tilde{\Pi}(\beta^\top x_i \geq \beta^\top x_j)$, where $i \neq j$. To illustrate the application, we split patients into low and high risk groups based on the estimated prognostic index, $\hat{\eta}_i = \hat{\beta}^\top x_i$, where $\hat{\beta}$ is the posterior mean. Patients with prognostic index less than the median (computed for the training set) are considered low risk, whilst patients with prognostic index greater than or equal to the median are considered high risk. The Kaplan-Meier (KM) curves for these groups are shown in Figure 2 (A). Critically, Bayesian approaches that only compute the MAP of β are only able to provide a point estimates for $\hat{\eta}$. In turn, our method is able to provide uncertainty around this quantity and therefore with respect to the ranking of the patients. For instance, in Figure 2 (B) we present the posterior probabilities comparing the risks between patients. We observe that the highest risk patients in the low risk group are comparable to the lowest risk patients in the high risk group, and that the highest risk patients within the high risk group are with high probability more at risk than the patients within the low risk group.

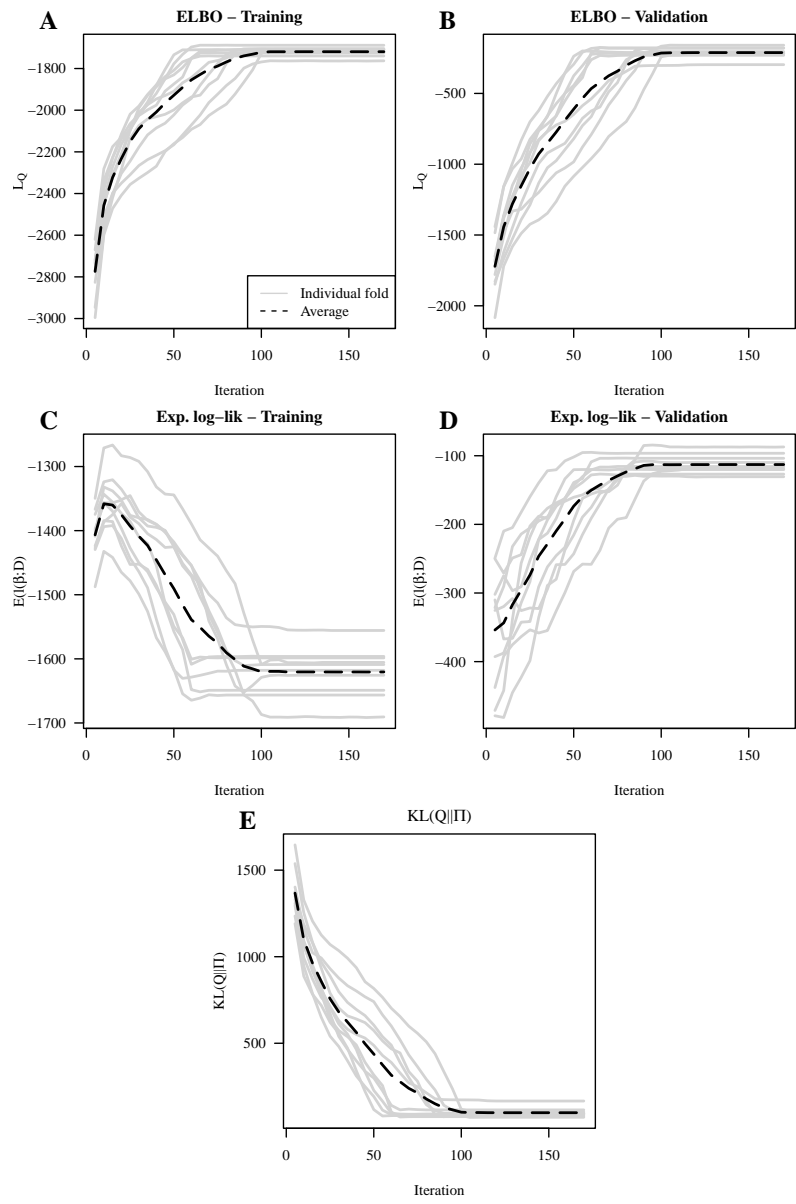


Figure 1: Ovarian cancer dataset model convergence diagnostics for $\lambda = 1$.

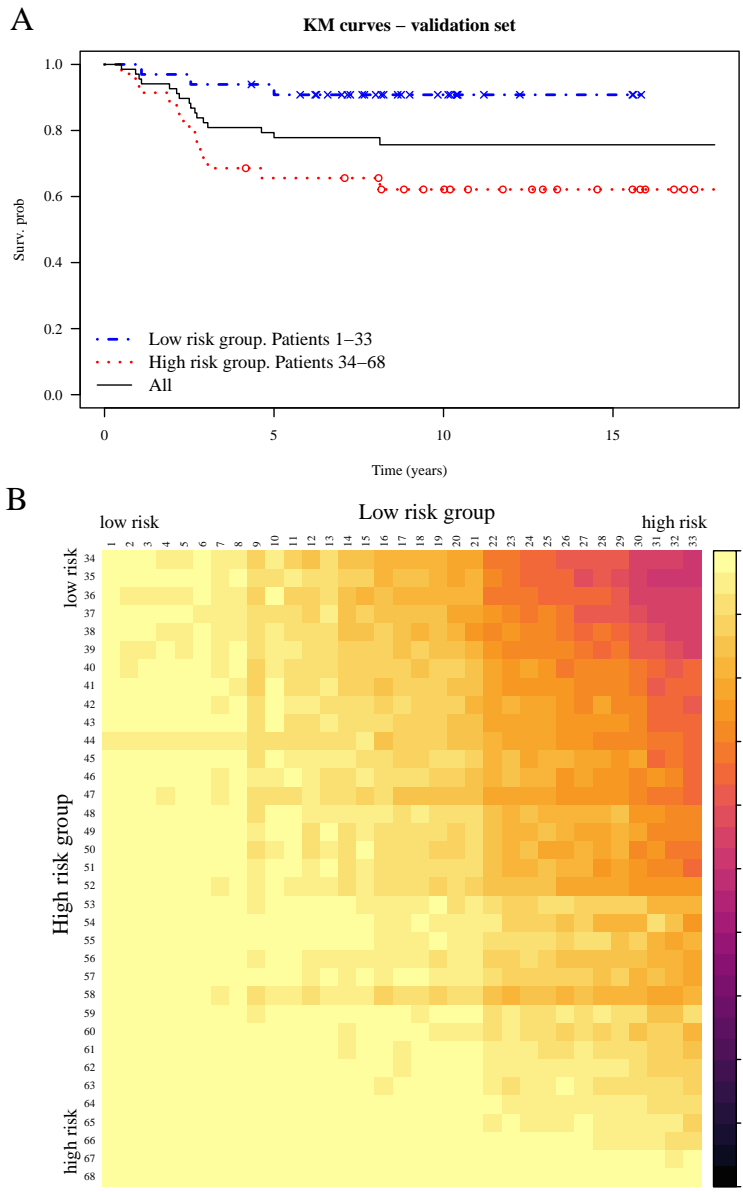


Figure 2: **(A)** Kaplan-Meier curves for patients in low and high risk groups. **(B)** Comparison of patients in the low and high risk groups (ordered by $\hat{\eta}$) – within each cell the (variational) posterior probability patient in row i is at greater risk than patient in column j is computed. Samples are taken from the second validation fold and the fit with $\lambda = 2.5$ is used.

5 Discussion

Variable selection and effect estimation for high-dimensional survival data has been an issue of great interest in recent years, particularly given the ever growing production of large scale omics data. However, the high-dimensionality and heterogeneity in the predictors, alongside the censoring in the response, makes the analysis a non-trivial task. While many recent methods have tackled these issues through a Bayesian approach, due to long compute times they often only produce point estimates rather than the full posterior and thereby fall short in providing the full Bayesian machinery.

We have bridged this gap and developed a scalable and interpretable mean-field variational approximation for Bayesian proportional hazards models with a spike-and-slab prior. We have demonstrated that the resulting variational posterior displays similar performance to the posterior obtained via MCMC whilst requiring a fraction of the compute time. Furthermore, we have demonstrated via an extensive simulation study that our proposed method performs comparably to state-of-the art Bayesian variable selection methods.

Finally, we have demonstrated that our method can be used for variable selection on two real world transcriptomics datasets, giving rise to results with pre-existing biological interpretations, thereby validating the practical utility of our method. We have also shown that the risk of patients can be compared through (variational) posterior probabilities, highlighting that the availability of a posterior distribution can be a powerful inferential tool. For illustrative purposes we examined the pairwise probabilities of patients grouped based on the prognostic index, however, patients could have alternatively been compared to other baselines e.g. the feature vector corresponding to median prognostic index. Furthermore, although this is not an aspect we have considered, grouping based on: age, cancer status, stage etc. may yield insightful results for practitioners and bioinformaticians.

A natural extension of our work would be to develop approximations with relaxed independence assumptions by using a more flexible variational family (Ning, 2021). Finally, we would like to highlight that improving the uncertainty quantification is an active area of research in the general VI community, see e.g. (Jerfel et al., 2021).

Acknowledgements

We would like to thank the reviewers for their constructive suggestions and comments.

Funding

MK gratefully acknowledges funding provided by EPSRC's StatML CDT, Imperial's CRUK centre and Imperial's Experimental Cancer Medicine centre.

Conflict of interest

The authors declare they have no competing interests.

References

- A. Antoniadis, P. Fryzlewicz, and F. Letué. The Dantzig Selector in Cox's Proportional Hazards Model. *Scandinavian Journal of Statistics*, 37(4):531–552, 2010. ISSN 14679469. doi: 10.1111/j.1467-9469.2009.00685.x.
- R. Bai, V. Rockova, and E. I. George. Spike-and-Slab Meets LASSO: A Review of the Spike-and-Slab LASSO, 2021. URL <http://arxiv.org/abs/2010.06451>.
- S. Banerjee, I. Castillo, and S. Ghosal. Bayesian inference in high-dimensional models, 2021. URL <http://arxiv.org/abs/2101.04491>.
- A. Bhadra, J. Datta, N. G. Polson, and B. Willard. Lasso meets horseshoe: A survey. *Stat. Sci.*, 34(3):405–427, 2019. ISSN 21688745. doi: 10.1214/19-STS700.
- C. M. Bishop. *Pattern Recognition and Machine Learning*. Springer, 2006.
- D. M. Blei and J. D. Lafferty. A correlated topic model of Science. *Ann. Appl. Stat.*, 1(1):17–35, 2007. ISSN 1932-6157. doi: 10.1214/07-aos114.
- D. M. Blei, A. Kucukelbir, and J. D. McAuliffe. Variational Inference: A Review for Statisticians. *Journal of the American Statistical Association*, 112(518):859–877, 2017. ISSN 1537274X. doi: 10.1080/01621459.2017.1285773.

- H. M. Bøvelstad, S. Nygård, H. L. Størvold, M. Aldrin, Borgan, A. Frigessi, and O. C. Lingjærde. Predicting survival from microarray data - A comparative study. *Bioinformatics*, 23(16):2080–2087, 2007. ISSN 13674803. doi: 10.1093/bioinformatics/btm305.
- R. Brent. *Algorithms for minimization without derivatives*. Prentice-Hall, 1973. ISBN 0-13-022335-2.
- P. Carbonetto and M. Stephens. Scalable variational inference for bayesian variable selection in regression, and its accuracy in genetic association studies. *Bayesian Analysis*, 7(1):73–108, 2012. ISSN 19360975. doi: 10.1214/12-BA703.
- C. M. Carvalho, N. G. Polson, and J. G. Scott. The horseshoe estimator for sparse signals. *Biometrika*, 97(2):465–480, 2010. ISSN 00063444. doi: 10.1093/biomet/asq017.
- I. Castillo and A. van der Vaart. Needles and straw in a haystack: posterior concentration for possibly sparse sequences. *Ann. Statist.*, 40(4):2069–2101, 2012. ISSN 0090-5364. doi: 10.1214/12-AOS1029. URL <https://doi.org/10.1214/12-AOS1029>.
- T. G. Clark, M. J. Bradburn, S. B. Love, and D. G. Altman. Survival Analysis Part I: Basic concepts and first analyses. *British Journal of Cancer*, 89(2):232–238, 2003. ISSN 00070920. doi: 10.1038/sj.bjc.6601118.
- A. Clauss, V. Ng, J. Liu, H. Piao, M. Russo, N. Vena, Q. Sheng, M. S. Hirsch, T. Bonome, U. Matulonis, A. H. Ligon, M. J. Birrer, and R. Drapkin. Overexpression of elafin in ovarian carcinoma is driven by genomic gains and activation of the nuclear factor κ B pathway and is associated with poor overall survival. *Neoplasia*, 12(2):161–172, 2010. ISSN 14765586. doi: 10.1593/neo.91542.
- D. R. Cox. Regression Models and Life-Tables. *Journal of the Royal Statistical Society, Series B*, 34(2):187–220, 2 1972. URL <http://www.ncbi.nlm.nih.gov/pubmed/2985181>.
- D. R. Cox. Partial Likelihood. *Biometrika*, 62(2):269–276, 2 1975.
- N. Depraetere and M. Vandebroek. A comparison of variational approximations for fast inference in mixed logit models. *Computational Statistics*, 32(1):93–125, 2017. ISSN 16139658. doi: 10.1007/s00180-015-0638-y.

- J. Fric, T. Zelante, A. Y. Wong, A. Mertes, H. B. Yu, and P. Ricciardi-Castagnoli. NFAT control of innate immunity. *Blood*, 120(7):1380–1389, 2012. ISSN 15280020. doi: 10.1182/blood-2012-02-404475.
- E. I. George and R. E. McCulloch. Variable Selection via Gibbs Sampling. *Journal of the American Statistical Association*, 88(423):881–889, 1993.
- M. Gonen and G. Heller. Concordance probability and discriminatory power in proportional hazards regression. *Biometrika*, 92(4):965–970, 2005.
- J. Gui and H. Li. Penalized Cox regression analysis in the high-dimensional and low-sample size settings, with applications to microarray gene expression data. *Bioinformatics*, 21(13):3001–3008, 2005. ISSN 13674803. doi: 10.1093/bioinformatics/bti422.
- J. Harrell, Frank E., R. M. Califf, D. B. Pryor, K. L. Lee, and R. A. Rosati. Evaluating the yield of medical tests. *JAMA*, 247(18):2543–2546, 05 1982. ISSN 0098-7484. doi: 10.1001/jama.1982.03320430047030. URL <https://doi.org/10.1001/jama.1982.03320430047030>.
- J. G. Ibrahim, M.-H. Chen, and D. Sinha. *Bayesian Survival Analysis*. Springer, 2001. ISBN 978-1-4757-3447-8.
- B. Izar, I. Tirosh, E. H. Stover, I. Wakiro, M. S. Cuoco, I. Alter, C. Rodman, R. Leeson, M.-J. Su, P. Shah, M. Iwanicki, S. R. Walker, A. Kanodia, J. C. Melms, S. Mei, J.-R. Lin, C. B. M. Porter, M. Slyper, J. Waldman, L. Jerby-Arnon, O. Ashenberg, T. J. Brinker, C. Mills, M. Rogava, S. Vigneau, P. K. Sorger, L. A. Garraway, P. A. Konstantinopoulos, J. F. Liu, U. Matulonis, B. E. Johnson, O. Rozenblatt-Rosen, A. Rotem, and A. Regev. A single-cell landscape of high-grade serous ovarian cancer. *Nature Medicine*, 26(8):1271–1279, aug 2020. ISSN 1078-8956. doi: 10.1038/s41591-020-0926-0. URL <http://www.nature.com/articles/s41591-020-0926-0>.
- T. S. Jaakkola and M. I. Jordan. A variational approach to Bayesian logistic regression models and their extensions, 1996.
- G. Jerfel, S. Wang, C. Fannjiang, K. A. Heller, Y. Ma, and M. I. Jordan. Variational Refinement for Importance Sampling Using the Forward Kullback-Leibler Divergence. In *Uncertainty in Artificial Intelligence - Proceedings of the 37th Conference, UAI 2021*, 06 2021. URL <http://arxiv.org/abs/2106.15980>.

- J. D. Kalbfleisch. Bayesian Analysis of Survival Time Data. *Journal of the Royal Statistical Society, Series B*, 40(2):214–221, 1978.
- A. Klami, S. Virtanen, E. Leppaaho, and S. Kaski. Group Factor Analysis. *IEEE Trans. Neural Networks Learn. Syst.*, 26(9):2136–2147, 2015. ISSN 21622388. doi: 10.1109/TNNLS.2014.2376974.
- D. A. Knowles and T. P. Minka. Non-conjugate Variational Message Passing for multinomial and binary regression. In *Adv. Neural Inf. Process. Syst. 24 25th Annu. Conf. Neural Inf. Process. Syst. 2011, NIPS 2011*, pages 1–9, 2011. ISBN 9781618395993.
- A. Lewin, L. Bottolo, and S. Richardson. Bayesian Methods for Gene Expression Analysis. In *Handb. Stat. Genomics*, volume 2, pages 843–40. Wiley, 07 2019. doi: 10.1002/9781119487845.ch30. URL <https://onlinelibrary.wiley.com/doi/10.1002/9781119487845.ch30>.
- F. Li and N. R. Zhang. Bayesian variable selection in structured high-dimensional covariate spaces with applications in genomics. *J. Am. Stat. Assoc.*, 105(491):1202–1214, 2010. ISSN 01621459. doi: 10.1198/jasa.2010.tm08177. URL <https://doi.org/10.1198/jasa.2010.tm08177>.
- G. Lightbody, V. Haberland, F. Browne, L. Taggart, H. Zheng, E. Parkes, and J. K. Blayney. Review of applications of high-throughput sequencing in personalized medicine: Barriers and facilitators of future progress in research and clinical application. *Brief. Bioinform.*, 20(5):1795–1811, 2019. ISSN 14774054. doi: 10.1093/bib/bby051.
- K. L. Lloyd, I. A. Cree, and R. S. Savage. Prediction of resistance to chemotherapy in ovarian cancer: A systematic review. *BMC Cancer*, 15(1):1–32, 2015. ISSN 14712407. doi: 10.1186/s12885-015-1101-8.
- B. A. Logsdon, G. E. Hoffman, and J. G. Mezey. A variational Bayes algorithm for fast and accurate multiple locus genome-wide association analysis. *BMC Bioinformatics*, 11, 2010. ISSN 14712105. doi: 10.1186/1471-2105-11-58.
- H. Lu, P. Cunnea, K. Nixon, N. Rinne, E. O. Aboagye, and C. Fotopoulou. Discovery of a biomarker candidate for surgical stratification in high-grade serous ovarian cancer. *Br. J. Cancer*, 124(7):1286–1293, 2021. ISSN 15321827. doi: 10.1038/s41416-020-01252-2. URL <http://dx.doi.org/10.1038/s41416-020-01252-2>.

- A. K. Maity, A. Bhattacharya, B. K. Mallick, and V. Baladandayuthapani. Bayesian data integration and variable selection for pan-cancer survival prediction using protein expression data. *Biometrics*, 76(1):316–325, 2020. ISSN 15410420. doi: 10.1111/biom.13132.
- J. C. Mar, N. A. Matigian, A. Mackay-Sim, G. D. Mellick, C. M. Sue, P. A. Silburn, J. J. McGrath, J. Quackenbush, and C. A. Wells. Variance of gene expression identifies altered network constraints in neurological disease. *PLoS Genetics*, 7(8), 2011. ISSN 15537390. doi: 10.1371/journal.pgen.1002207.
- T. J. Mitchell and J. J. Beauchamp. Bayesian variable selection in linear regression. *Journal of the American Statistical Association*, 83(404):1023–1032, 1988. ISSN 1537274X. doi: 10.1080/01621459.1988.10478694.
- A. A. Mourskaia, E. Amir, Z. Dong, K. Tiedemann, S. Cory, A. Omeroglu, N. Bertos, V. Ouellet, M. Clemons, G. L. Scheffer, M. Park, M. Hallett, S. V. Komarova, and P. M. Siegel. ABCC5 supports osteoclast formation and promotes breast cancer metastasis to bone. *Breast Cancer Research*, 14(6):1–16, 2012. ISSN 14655411. doi: 10.1186/bcr3361.
- S. A. Murphy and A. W. Van Der Vaart. On profile likelihood. *J. Am. Stat. Assoc.*, 95(450):449–465, 2000. ISSN 1537274X. doi: 10.1080/01621459.2000.10474219.
- M. A. Newton, A. Noueiry, D. Sarkar, and P. Ahlquist. Detecting differential gene expression with a semiparametric hierarchical mixture method. *Biostatistics*, 5(2):155–176, 2004. ISSN 14654644. doi: 10.1093/biostatistics/5.2.155.
- A. Nikooienejad, W. Wang, and V. E. Johnson. Bayesian variable selection for survival data using inverse moment priors. *Annals of Applied Statistics*, 14(2):809–828, 2020. ISSN 19417330. doi: 10.1214/20-AOAS1325.
- B. Ning. Spike and slab Bayesian sparse principal component analysis, 2021. URL <http://arxiv.org/abs/2102.00305>.
- D. J. Nott, S. L. Tan, M. Villan, and R. Kohn. Regression density estimation with variational methods and stochastic approximation. *Journal of Computational and Graphical Statistics*, 21(3):797–820, 2012. ISSN 10618600. doi: 10.1080/10618600.2012.679897.

- R. B. O’Hara and M. J. Sillanpää. A review of bayesian variable selection methods: What, how and which. *Bayesian Anal.*, 4(1):85–118, 2009. ISSN 19360975. doi: 10.1214/09-BA403.
- M. Opper and C. Arachambeau. The Variational Gaussian Approximaiton Revisited, 2009.
- J. T. Ormerod, C. You, and S. Müller. A variational bayes approach to variable selection. *Electron. J. Stat.*, 11(2):3549–3594, 2017. ISSN 19357524. doi: 10.1214/17-EJS1332.
- P. Papastamoulis, J. Hensman, P. Glaus, and M. Rattray. Improved variational Bayes inference for transcript expression estimation. *Statistical Applications in Genetics and Molecular Biology*, 13(2):203–216, 2014. ISSN 15446115. doi: 10.1515/sagmb-2013-0054.
- S. A. Park, N. J. Sung, B. J. Choi, W. Kim, S. H. Kim, and Y. J. Surh. Gremlin-1 augments the oestrogen-related receptor α signalling through EGFR activation: implications for the progression of breast cancer. *British Journal of Cancer*, 123(6):988–999, 2020. ISSN 15321827. doi: 10.1038/s41416-020-0945-0. URL <http://dx.doi.org/10.1038/s41416-020-0945-0>.
- T. Park and G. Casella. The Bayesian Lasso. *J. Am. Stat. Assoc.*, 103(482):681–686, 2008. ISSN 01621459. doi: 10.1198/016214508000000337.
- A. Planche, M. Bacac, P. Provero, C. Fusco, M. Delorenzi, J. C. Stehle, and I. Stamenkovic. Identification of prognostic molecular features in the reactive stroma of human breast and prostate cancer. *PLoS ONE*, 6(5), 2011. ISSN 19326203. doi: 10.1371/journal.pone.0018640.
- K. Ray and B. Szabó. Variational Bayes for High-Dimensional Linear Regression With Sparse Priors. *Journal of the American Statistical Association*, pages 1–12, 01 2021. ISSN 0162-1459. doi: 10.1080/01621459.2020.1847121. URL <https://www.tandfonline.com/doi/full/10.1080/01621459.2020.1847121><http://dx.doi.org/10.1080/01621459.2020.1847121>.
- K. Ray, B. Szabo, and G. Clara. Spike and slab variational Bayes for high dimensional logistic regression. In H. Larochelle, M. Ranzato, R. Hadsell, M. F. Balcan, and H. Lin, editors, *Adv. Neural Inf. Process. Syst.*, volume 33, pages 14423–14434. Curran Associates, Inc., 2020. URL <https://proceedings.neurips.cc/paper/2020/file/a5bad363fc47f424ddf5091c8471480a-Paper.pdf>.
- Y. Rivera-Rivera, M. Marina, S. Jusino, M. Lee, J. V. Velázquez, C. Chardón-Colón, G. Vargas, J. Padmanabhan, S. P. Chellappan, and H. I. Saavedra. The Nek2 centrosome-mitotic kinase

- contributes to the mesenchymal state, cell invasion, and migration of triple-negative breast cancer cells. *Scientific reports*, 11(1):9016, 2021. ISSN 20452322. doi: 10.1038/s41598-021-88512-0. URL <https://doi.org/10.1038/s41598-021-88512-0>.
- N. Simon, J. Friedman, T. Hastie, and R. Tibshirani. Regularization paths for cox’s proportional hazards model via coordinate descent. *Journal of Statistical Software*, 39(5):1–13, 2011. URL <https://www.jstatsoft.org/v39/i05/>.
- V. Svensson, A. Gayoso, N. Yosef, and L. Pachter. Interpretable factor models of single-cell RNA-seq via variational autoencoders. *Bioinformatics*, 36(11):3418–3421, 2020. ISSN 14602059. doi: 10.1093/bioinformatics/btaa169.
- Z. Tang, Y. Shen, X. Zhang, and N. Yi. The spike-and-slab lasso Cox model for survival prediction and associated genes detection. *Bioinformatics*, 33(18):2799–2807, 2017. ISSN 14602059. doi: 10.1093/bioinformatics/btx300.
- TCGA. The cancer genome atlas program - national cancer institute. <https://www.cancer.gov/tcga>, 2022. (Accessed on 24/03/2022).
- A. E. Teschendorff, Y. Wang, N. L. Barbosa-Morais, J. D. Brenton, and C. Caldas. A variational Bayesian mixture modelling framework for cluster analysis of gene-expression data. *Bioinformatics*, 21(13):3025–3033, 2005. ISSN 13674803. doi: 10.1093/bioinformatics/bti466.
- R. Tibshirani. Regression Shrinkage and Selection via the Lasso. *Journal of the Royal Statistical Society, Series B*, 58(1):267–288, 1996.
- R. Tibshirani. The lasso method for variable selection in the cox model. *Stat. Med.*, 16(4):385–395, 1997. ISSN 02776715. doi: 10.1002/(SICI)1097-0258(19970228)16:4<385::AID-SIM380>3.0.CO;2-3.
- M. Titsias and M. Lázaro-Gredilla. Spike and slab variational inference for multi-task and multiple kernel learning. In J. Shawe-Taylor, R. Zemel, P. Bartlett, F. Pereira, and K. Q. Weinberger, editors, *Advances in Neural Information Processing Systems*, volume 24. Curran Associates, Inc., 2011. URL <https://proceedings.neurips.cc/paper/2011/file/b495ce63ede0f4efc9eec62cb947c162-Paper.pdf>.

- W. Widłak. *Molecular Biology*. Springer Berlin Heidelberg, 2013.
- D. M. Witten and R. Tibshirani. Survival analysis with high-dimensional covariates. *Stat. Methods Med. Res.*, 19(1):29–51, 2010.
- B. Xin, K. Q. Ji, Y. S. Liu, and X. D. Zhao. Higher expression of calcineurin predicts poor prognosis in unique subtype of ovarian cancer. *Journal of Ovarian Research*, 12(1):1–12, 2019. ISSN 17572215. doi: 10.1186/s13048-019-0550-0.
- C. Yau, L. Esserman, D. H. Moore, F. Waldman, J. Sninsky, and C. C. Benz. A multigene predictor of metastatic outcome in early stage hormone receptor-negative and triple-negative breast cancer. *Breast Cancer Research*, 12(5), 2010. ISSN 14655411. doi: 10.1186/bcr2753.
- C. Zhang, J. Butepage, H. Kjellstrom, and S. Mandt. Advances in Variational Inference. *IEEE Trans. Pattern Anal. Mach. Intell.*, 41(8):2008–2026, 2019. ISSN 19393539. doi: 10.1109/TPAMI.2018.2889774.
- F. Zhang and P. Flaherty. Variational inference for rare variant detection in deep, heterogeneous next-generation sequencing data. *BMC Bioinformatics*, 18(1):1–10, 2017. ISSN 14712105. doi: 10.1186/s12859-016-1451-5. URL <http://dx.doi.org/10.1186/s12859-016-1451-5>.
- H. Zou and T. Hastie. Regularization and variable selection via the elastic net. *J. R. Stat. Soc. Ser. B (Statistical Methodol.)*, 67(5):768–768, 11 2005. ISSN 1369-7412. doi: 10.1111/j.1467-9868.2005.00527.x. URL <https://onlinelibrary.wiley.com/doi/10.1111/j.1467-9868.2005.00527.x>.

A Variational algorithm

Recall that our mean-field variational family is given by

$$\mathcal{Q} = \left\{ Q_{\mu, \sigma, \gamma} = \bigotimes_{j=1}^p [\gamma_j N(\mu_j, \sigma_j^2) + (1 - \gamma_j) \delta_0] : \mu_j \in \mathbb{R}, \sigma_j \in \mathbb{R}^+, \gamma_j \in [0, 1] \right\}, \quad (12)$$

and the posterior is given by

$$d\Pi(\beta|\mathcal{D}) = \Pi_D^{-1} e^{l_p(\mathcal{D};\beta)} d\Pi(\beta), \quad (13)$$

where $l_p = \log L_p$ is the log (partial) likelihood and Π_D is the normalising constant. Our aim is to evaluate the KL divergence between an element $Q_{\mu, \sigma, \gamma}$ of the variational family and the posterior $\Pi(\cdot|\mathcal{D})$ as a function of μ_j, σ_j and γ_j , whilst keeping all other parameters fixed. Due to the discrete components of the prior (4), one has to be careful with the different terms since they may not be absolutely continuous with respect to one another (as measures), and hence may not have densities.

A.1 Update equations for μ_j and σ_j

We first compute the KL divergence between $Q_{\mu, \sigma, \gamma}$ and the posterior $\Pi(\cdot|\mathcal{D})$, conditional on $z_j = 1$, as a function of μ_j and σ_j . We recall the notation μ_{-j} , which refers to all the components of (μ_1, \dots, μ_p) except μ_j . Firstly, since both the prior (4) and variational family (6) consist of factorisable distributions, the Radon-Nikodym derivative between them also factorizes

$$\frac{dQ_{\mu, \sigma, \gamma}}{d\Pi}(\beta) = \prod_{j=1}^n \frac{dQ_j}{d\Pi_j}(\beta_j), \quad (14)$$

where $Q_j = \gamma_j N(\mu_j, \sigma_j^2) + (1 - \gamma_j) \delta_0$ and $\Pi_j = \bar{w} \text{Lap}(\lambda) + (1 - \bar{w}) \delta_0$ with $\bar{w} = a_0 / (a_0 + b_0)$. The latter expression for the prior follows from integrating out the hierarchical representation (4), whereupon we have weights equal to the prior mean weight \bar{w} .

Since the variational probability distribution of β_j conditional on $z_j = 1$ (i.e. the slab component) is singular with respect to the Dirac measure δ_0 , in this case it is sufficient to consider only the continuous part of the prior measure in the denominator of the Radon-Nikodym derivative, that is

$$\frac{dQ_{\mu_j, \sigma_j | z_j=1}}{d\Pi_j}(\beta_j) = \frac{dN(\mu_j, \sigma_j^2)}{\bar{w} d\text{Lap}(\lambda)}(\beta_j).$$

Using the above facts, $\text{KL}(Q_{\mu,\sigma,\gamma|z_j=1} \parallel \Pi(\cdot|\mathcal{D}))$ equals, as a function of μ_j and σ_j ,

$$\begin{aligned}
\mathbb{E}_{\mu,\sigma,\gamma|z_j=1} \left[\log \frac{dQ}{d\Pi(\cdot|\mathcal{D})} \right] &= \mathbb{E}_{\mu,\sigma,\gamma|z_j=1} \left[\log \frac{dQ_{\mu,\sigma,\gamma}}{d\Pi} - l_p(\mathcal{D}; \beta) + \log \Pi_D \right] \\
&= \mathbb{E}_{\mu,\sigma,\gamma|z_j=1} \left[\log \left(\frac{dN(\mu_j, \sigma_j^2)}{\bar{w}d\text{Lap}(\lambda)}(\beta_j) \prod_{k \neq j} \frac{dQ_k}{d\Pi_k}(\beta_k) \right) - l_p(\mathcal{D}; \beta) + \log \Pi_D \right] \\
&= \mathbb{E}_{\mu,\sigma,\gamma|z_j=1} \left[\log \left(\prod_{k \neq j} \frac{dQ_k}{d\Pi_k}(\beta_k) \right) + \log \left(\frac{1}{\sqrt{2\pi\sigma_j^2}} e^{-\frac{(\beta_j - \mu_j)^2}{2\sigma_j^2}} \frac{2}{\lambda \bar{w}} e^{\lambda|\beta_j|} \right) - l_p(\mathcal{D}; \beta) + \log \Pi_D \right] \\
&= \mathbb{E}_{\mu,\sigma,\gamma|z_j=1} \left[\lambda|\beta_j| - \log \sigma_j - \frac{(\beta_j - \mu_j)^2}{2\sigma_j^2} - l_p(\mathcal{D}; \beta) \right] + C \\
&= \mathbb{E}_{\mu,\sigma,\gamma|z_j=1} \left[\lambda|\beta_j| - \log \sigma_j - \frac{(\beta_j - \mu_j)^2}{2\sigma_j^2} - \sum_{\{i:\delta_i=1\}} \left(\beta^\top x_i - \log \sum_{r \in R(t_i)} \exp(\beta^\top x_r) \right) \right] + C,
\end{aligned}$$

where the constant C is independent of μ_j and σ_j and may vary from line to line. Since $|\beta_j|$ has a folded normal distribution, it has expectation $\sigma_j \sqrt{2/\pi} e^{-\mu_j^2/(2\sigma_j^2)} + \mu_j(1 - 2\Phi(-\mu_j/\sigma_j))$, where Φ is the CDF of the standard normal distribution. The previous display equals

$$\begin{aligned}
&\sum_{\{i:\delta_i=1\}} \left(\mathbb{E}_{\mu,\sigma,\gamma|z_j=1} \left[\log \sum_{r \in R(t_i)} \exp(\beta^\top x_r) \right] - \mu_j x_{ij} \right) \\
&\quad + \lambda \sigma_j \sqrt{2/\pi} e^{-\mu_j^2/(2\sigma_j^2)} + \lambda \mu_j (1 - 2\Phi(-\mu_j/\sigma_j)) - \log \sigma_j + C \\
&\leq \sum_{\{i:\delta_i=1\}} \left(\log \sum_{r \in R(t_i)} \mathbb{E}_{\mu,\sigma,\gamma|z_j=1} [\exp(\beta^\top x_r)] - \mu_j x_{ij} \right) \\
&\quad + \lambda \sigma_j \sqrt{2/\pi} e^{-\mu_j^2/(2\sigma_j^2)} + \lambda \mu_j (1 - 2\Phi(-\mu_j/\sigma_j)) - \log \sigma_j + C \\
&= \sum_{\{i:\delta_i=1\}} \left(\log \sum_{r \in R(t_i)} M(x_{rj}, \mu_j, \sigma_j) P_j(x_r, \mu, \sigma, \gamma) - \mu_j x_{ij} \right) \\
&\quad + \lambda \sigma_j \sqrt{2/\pi} e^{-\mu_j^2/(2\sigma_j^2)} + \lambda \mu_j (1 - 2\Phi(-\mu_j/\sigma_j)) - \log \sigma_j + C, \tag{15}
\end{aligned}$$

where $M(x_{rj}, \mu_j, \sigma_j) = \exp(\mu_j x_{rj} + \frac{1}{2} \sigma_j^2 x_{rj}^2)$ and $P_j(x_r, \mu, \sigma, \gamma) = \prod_{k \neq j} (\gamma_k M(x_{rk}, \mu_k, \sigma_k) + (1 - \gamma_k))$ and we have used Jensen's inequality. Noting, to evaluate an expression for $\mathbb{E}_{\mu,\sigma,\gamma|z_j=1} [e^{\beta^\top x_r}]$ we exploit the independence structure of β , i.e. $\beta_j \stackrel{\text{ind}}{\sim} \gamma_j N(\mu_j, \sigma_j^2) + (1 - \gamma_j) \delta_0$, and hence $\mathbb{E}_{\mu,\sigma,\gamma|z_j=1} [e^{\beta^\top x_r}] = \mathbb{E}_{\mu_j, \sigma_j, \gamma_j|z_j=1} [e^{\beta_j x_{rj}}] \prod_{k \neq j} \mathbb{E}_{\mu_k, \sigma_k, \gamma_k} [e^{\beta_k x_{rk}}]$.

The last display thus provides an upper bound for the KL divergence and hence a surrogate objective function. Minimising this expression with respect to either μ_j or σ_j gives the same minimisers as minimising the objective functions (8) or (9), respectively, and hence gives our update equations.

A.2 Update equation for γ_j

In a similar way, the KL divergence between $Q_{\mu,\sigma,\gamma}$ and $\Pi(\cdot|\mathcal{D})$ as of function of γ_j equals

$$\mathbb{E}_{\mu,\sigma,\gamma} \left[\log \left(\prod_{k \neq j} \frac{dQ_k}{d\Pi_k}(\beta_k) \right) + \log \frac{d[\gamma_j N(\mu_j, \sigma_j^2) + (1 - \gamma_j)\delta_0]}{d[\bar{w}\text{Lap}(\lambda) + (1 - \bar{w})\delta_0]}(\beta_j) - l_p(\mathcal{D}; \beta) \right] + C.$$

We now split this expression in terms of the events $z_j = 1$ or 0 . Noting that with $Q_{\mu,\sigma,\gamma}$ -probability one, $\beta_j = 0$ if and only if $z_j = 0$, the last display can be rewritten as

$$\begin{aligned} & \mathbb{E}_{\mu,\sigma,\gamma} \left[\mathbb{I}_{\{z_j=1\}} \log \frac{\gamma_j dN(\mu_j, \sigma_j^2)}{\bar{w} d\text{Lap}(\lambda)}(\beta_j) + \mathbb{I}_{\{z_j=0\}} \log \frac{(1 - \gamma_j)}{(1 - \bar{w})} - l_p(\mathcal{D}; \beta) \right] + C \\ &= \mathbb{E}_{\mu,\sigma,\gamma} \left[\mathbb{I}_{\{z_j=1\}} \left(\log \left(\frac{\gamma_j}{\bar{w}} \frac{\sqrt{2}}{\sqrt{\pi}\sigma_j\lambda} \right) + \lambda|\beta_j| - \frac{(\beta_j - \mu_j)^2}{2\sigma_j^2} \right) + \mathbb{I}_{\{z_j=0\}} \log \frac{(1 - \gamma_j)}{(1 - \bar{w})} - l_p(\mathcal{D}; \beta) \right] + C \\ &= \gamma_j \left\{ \log \frac{\gamma_j}{\bar{w}} + \log \frac{\sqrt{2}}{\sqrt{\pi}\sigma_j\lambda} + \lambda\sigma_j\sqrt{2/\pi}e^{-\mu_j^2/(2\sigma_j^2)} + \lambda\mu_j(1 - 2\Phi(-\mu_j/\sigma_j)) - \frac{1}{2} \right\} \\ & \quad + (1 - \gamma_j) \log \frac{(1 - \gamma_j)}{(1 - \bar{w})} + \sum_{\{i:\delta_i=1\}} \left(\mathbb{E}_{\mu,\sigma,\gamma} \left[\log \sum_{r \in R(t_i)} \exp(\beta^\top x_r) \right] - \gamma_j \mu_j x_{ij} \right) + C, \end{aligned}$$

where C does not depend on γ_j . Upper bounding the expectation in the last display using Jensen's inequality,

$$\begin{aligned} & \mathbb{E}_{\mu,\sigma,\gamma} \left[\log \sum_{r \in R(t_i)} \exp(\beta^\top x_r) \right] \\ &= \sum_{\{i:\delta_i=1\}} \left(\gamma_j \mathbb{E}_{N(\mu_j, \sigma_j^2) \otimes Q_{-j}} \left[\log \sum_{r \in R(t_i)} e^{\beta^\top x_r} \right] + (1 - \gamma_j) \mathbb{E}_{\delta_0 \otimes Q_{-j}} \left[\log \sum_{r \in R(t_i)} e^{\beta^\top x_r} \right] \right) \\ &\leq \sum_{\{i:\delta_i=1\}} \left(\gamma_j \log \sum_{r \in R(t_i)} \mathbb{E}_{N(\mu_j, \sigma_j^2) \otimes Q_{-j}} \left[e^{\beta^\top x_r} \right] + (1 - \gamma_j) \log \sum_{r \in R(t_i)} \mathbb{E}_{\delta_0 \otimes Q_{-j}} \left[e^{\beta^\top x_r} \right] \right) \end{aligned}$$

$$= \sum_{\{i:\delta_i=1\}} \left(\gamma_j \log \sum_{r \in R(t_i)} M(x_{rj}, \mu_j, \sigma_j) P_j(x_r, \mu, \sigma, \gamma) + (1 - \gamma_j) \log \sum_{r \in R(t_i)} P_j(x_r, \mu, \sigma, \gamma) \right).$$

Substituting this into the second to last display, we can upper bound the KL divergence as a function of γ_j by

$$\begin{aligned} & \gamma_j \sum_{\{i:\delta_i=1\}} \left(\log \sum_{r \in R(t_i)} M(x_{rj}, \mu_j, \sigma_j) P_j(x_r, \mu, \sigma, \gamma) - \log \sum_{r \in R(t_i)} P_j(x_r, \mu, \sigma, \gamma) - \mu_j x_{ij} \right) + \\ & \gamma_j \left(\lambda \sigma_j \sqrt{2/\pi} e^{-\mu_j^2/(2\sigma_j^2)} + \lambda \mu_j (1 - 2\Phi(-\mu_j/\sigma_j)) + \log \frac{\sqrt{2}}{\sqrt{\pi}\sigma_j\lambda} - \frac{1}{2} + \log \frac{\gamma_j}{1 - \gamma_j} - \log \frac{a_0}{b_0} \right) \quad (16) \\ & + \log(1 - \gamma_j) + C \end{aligned}$$

where C does not depend on γ_j and we have used $\bar{w} = a_0/(a_0 + b_0)$. Setting the derivative with respect to γ_j of the last equation equal to zero and rearranging gives the update equation (10) for γ_j .

B Goodness of fit measures

A commonly used measure of goodness of fit in the VI literature is the evidence lower bound (ELBO), which acts as a lower bound for the Bayesian marginal likelihood and is defined as

$$\mathcal{L}_Q = \mathbb{E}_Q [\log L_p] - \text{KL}(Q \parallel \Pi), \quad (17)$$

with $Q \in \mathcal{Q}$ (Bishop, 2006). Intuitively, the ELBO trades-off how well the model fits the data (first term) with how close it is to the prior (second term). Picking the parameter that maximizes the ELBO is the variational analogue of empirical Bayes, which selects parameters by maximising the marginal likelihood. Since VI is used exactly when the marginal likelihood is intractable, it is natural to use the ELBO, which measures the quality of the variational approximation (Bishop, 2006).

Similar to our derivation of the coordinate-ascent update expression for γ_j , we exploit the

product structure of our variational distribution to evaluate an expression for the ELBO.

$$\begin{aligned}
\mathcal{L}_Q &= -\mathbb{E}_{\mu,\sigma,\gamma} \left[\log \frac{dQ_{\mu,\sigma,\gamma}}{d\Pi}(\beta) - l_p(\mathcal{D}; \beta) \right] \\
&= -\mathbb{E}_{\mu,\sigma,\gamma} \left[\sum_{j=1}^p \left(\mathbb{I}_{\{z_j=1\}} \log \frac{\gamma_j dN(\mu_j, \sigma_j^2)}{\bar{w}_j d\text{Lap}(\lambda)}(\beta_j) + \mathbb{I}_{\{z_j=0\}} \log \frac{(1-\gamma_j)}{(1-\bar{w}_j)} \right) - l_p(\mathcal{D}; \beta) \right] \\
&= -\sum_{j=1}^p \left(\mathbb{E}_{Q_j} \left[\mathbb{I}_{\{z_j=1\}} \log \frac{\gamma_j dN(\mu_j, \sigma_j^2)}{\bar{w} d\text{Lap}(\lambda)}(\beta_j) + \mathbb{I}_{\{z_j=0\}} \log \frac{(1-\gamma_j)}{(1-\bar{w})} \right] \right) + \mathbb{E}_{\mu,\sigma,\gamma} [l_p(\mathcal{D}; \beta)] \\
&= -\sum_{j=1}^p \left(\gamma_j \left\{ \lambda \sigma_j \sqrt{2/\pi} e^{-\mu_j^2/(2\sigma_j^2)} + \lambda \mu_j (1 - 2\Phi(-\mu_j/\sigma_j)) \right\} + \log \frac{\sqrt{2}}{\sqrt{\pi} \sigma_j \lambda} - \frac{1}{2} \right. \\
&\quad \left. + \log \frac{\gamma_j}{1-\gamma_j} - \log \frac{a_0}{b_0} \right\} + \log(1-\gamma_j) - \log(1-\bar{w}) \Big) + \mathbb{E}_{\mu,\sigma,\gamma} [l_p(\mathcal{D}; \beta)] \tag{18}
\end{aligned}$$

As we cannot evaluate a closed-form expression for $\mathbb{E}_{\mu,\sigma,\gamma} [l_p(\mathcal{D}; \beta)]$, we use Monte Carlo integration to estimate this quantity, i.e. we compute

$$\hat{\mathcal{L}}_Q = \frac{1}{B} \sum_{i=1}^B \log L_p(\mathcal{D}; \beta^{(i)}) - \text{KL}(Q \parallel \Pi), \quad Q \in \mathcal{Q}, \tag{19}$$

where B are the number of Monte Carlo samples and $\beta^{(i)} \stackrel{\text{iid}}{\sim} Q$ for $i = 1, \dots, B$. Notably, the elements of $\beta^{(i)} = (\beta_1^{(i)}, \dots, \beta_p^{(i)})^\top \in \mathbb{R}^p$ are given by sampling $\beta_j^{(i)} \stackrel{\text{iid}}{\sim} N(\mu_j, \sigma_j^2)$ with probability γ_j or taking $\beta_j^{(i)} = 0$ with probability $1 - \gamma_j$ for $j = 1, \dots, p$. The remaining term can be evaluated explicitly as

$$\begin{aligned}
\text{KL}(Q \parallel \Pi) &= \sum_{j=1}^p \left(\gamma_j \left\{ \lambda \sigma_j \sqrt{\frac{2}{\pi}} e^{-\frac{\mu_j^2}{2\sigma_j^2}} + \log \frac{\sqrt{2}}{\sqrt{\pi} \sigma_j \lambda} - \frac{1}{2} \right. \right. \\
&\quad \left. \left. + \lambda \mu_j (1 - 2\Phi(-\frac{\mu_j}{\sigma_j})) + \log \frac{\gamma_j}{1-\gamma_j} - \log \frac{a_0}{b_0} \right\} + \log(1-\gamma_j) \right). \tag{20}
\end{aligned}$$

Although popular, model selection based on the ELBO is not justified theoretically and can be sensitive to the setting; therefore we consider additional goodness of fit measures. One such measure, proposed by [Nott et al. \(2012\)](#), involves using the variational posterior to approximate

the log-predictive density score (LPDS) on an held out testing dataset, defined as

$$\text{LPDS} = \log \int L_p(\mathcal{D}_{\text{test}}; \beta) d\tilde{\Pi}(\beta | \mathcal{D}_{\text{train}}) = \log \mathbb{E}_{\tilde{\Pi}} [L_p(\mathcal{D}_{\text{test}}; \beta)],$$

where $\mathcal{D}_{\text{test}}$ is the held out test set and $\mathcal{D}_{\text{train}}$ is the training set used to compute $\tilde{\Pi}$ (Nott et al., 2012). By Jensen's inequality,

$$\log \mathbb{E}_{\tilde{\Pi}} [L_p(\mathcal{D}_{\text{test}} | \beta)] \leq \mathbb{E}_{\tilde{\Pi}} [\log L_p(\mathcal{D}_{\text{test}} | \beta)]$$

Hence, given that computing the ELBO for a validation set involves computing $\mathbb{E}_{\tilde{\Pi}} [\log L_p(\mathcal{D}_{\text{test}}; \beta)]$, we can cheaply obtain an upper bound for the LPDS to use as a goodness of fit measure.

A further goodness of fit measure specific to survival models is the concordance index (c-index), defined as

$$k = \mathbb{P}(\mathbf{T}_i > \mathbf{T}_j | \eta_j > \eta_i), \quad i \neq j,$$

where $\eta_k = \beta_0^\top x_k$ is referred to as the *prognostic index*. Intuitively, for two observations $(t_i, \delta_i = 1, x_i)$ and $(t_j, \delta_j = 1, x_j)$, when $\eta_j > \eta_i$ we would expect $t_i > t_j$. This remark follows from the form of the hazard function under the PHM, where we assume $h(t) = h_0(t) \exp(\beta^\top x) = h_0(t) \exp(\eta)$. Therefore, when $\eta_j > \eta_i$ the hazard rate $h(t_j) > h(t_i)$ and thus we would expect t_j to have failed before t_i . Often the c-index is estimated by,

$$\hat{k} = \frac{\sum_{i=1}^n \sum_{j>i} \mathbb{I}(t_i < t_j) \mathbb{I}(\hat{\eta}_i > \hat{\eta}_j) \delta_i + \mathbb{I}(t_j < t_i) \mathbb{I}(\hat{\eta}_j > \hat{\eta}_i) \delta_j}{\sum_{i=1}^n \sum_{j>i} \mathbb{I}(t_i < t_j) \delta_i + \mathbb{I}(t_j < t_i) \delta_j},$$

where the prognostic index is estimated using $\hat{\eta}_j = \hat{\beta}^\top x_j$ for a given point estimate $\hat{\beta}$ of β , and $\mathbb{I}(\cdot)$ is the indicator function (Harrell et al., 1982). Notably, the c-index is not robust to censoring and tends to overestimate k when there is a high degree of censoring (Gonen and Heller, 2005).

C Simulation study

C.1 Markov chain Monte Carlo sampler

To construct our sampler we note that the model given by (5) can be reformulated such that the prior is given by:

$$\begin{aligned}\beta_j &\stackrel{\text{iid}}{\sim} \text{Laplace}(\lambda) \\ z_j|w_j &\stackrel{\text{iid}}{\sim} \text{Bernoulli}(w_j) \\ w_j &\stackrel{\text{iid}}{\sim} \text{Beta}(a_0, b_0)\end{aligned}\tag{21}$$

and likelihood as $p(\mathcal{D}|\beta, z) = L_p(\mathcal{D}; \beta \circ z)$ where \circ denotes the element wise product, i.e. $(\beta \circ z)_j = \beta_j z_j$.

Algorithm 2 details our Gibbs sampler for the posterior in (5) based on the above formulation. Notably, we introduce the notation $x_{k:l} := (x_i)_{i=k}^l$, for $1 \leq l < k \leq p$, $x \in \mathbb{R}^p$, and denote $\beta^{(i)} \in \mathbb{R}^p$, $z^{(i)} \in \{0, 1\}^p$ and $w^{(i)} \in [0, 1]^p$ as the MCMC samples.

Algorithm 2 Spike and Slab MCMC sampler

- 1: **Require:** K , the Metropolis-Hastings proposal kernel, N : number of samples.
 - 2: Initialise $z^{(0)}, \beta^{(0)}, w^{(0)}$
 - 3: **for** $i = 1, \dots, N$ **do**
 - 4: **for** $j = 1, \dots, p$
 - 5: $w_j^{(i)} \sim w_j | \mathcal{D}, \beta_{1:p}^{(i-1)}, z_{1:p}^{(i-1)}, w_{1:j-1}^{(i-1)}, w_{j+1:p}^{(i-1)}$
 - 6: **for** $j = 1, \dots, p$
 - 7: $z_j^{(i)} \sim z_j | \mathcal{D}, \beta_{1:p}^{(i-1)}, z_{1:(j-1)}^{(i)}, z_{(j+1):p}^{(i-1)}, w_{1:p}^{(i)}$
 - 8: **for** $j = 1, \dots, p$
 - 9: $\beta_j^{(i)} \sim \beta_j | \mathcal{D}, \beta_{1:(j-1)}^{(i-1)}, \beta_{(j+1):p}^{(i-1)}, z_{1:p}^{(i)}, w_{1:p}^{(i)}$
-

Ignoring the superscript for clarity, the distribution $w_j | \mathcal{D}, \beta, z, w_{-j}$ is conditionally independent of \mathcal{D}, β, z and w_{-j} . Therefore, $w_j^{(i)}$ is sampled iid. from the prior of w_j , i.e. $w_j^{(i)} \stackrel{\text{iid.}}{\sim} \text{Beta}(a_0, b_0)$. Regarding $z_j^{(i)}$, the conditional density

$$\begin{aligned}p(z_j | \mathcal{D}, \beta, z_{-j}, w) &\propto p(\mathcal{D} | \beta, z_{-j}, z_j, w) \pi(z_j | \beta, z_{-j}, w) \\ &= p(\mathcal{D}; \beta, z) \pi(z_j | w_j).\end{aligned}\tag{22}$$

As z_j is discrete, evaluating the RHS of (22) for $z_j = 0$ and $z_j = 1$, gives the unnormalised conditional probabilities. Summing gives the normalisation constant and thus we can sample z_j from a Bernoulli distribution with parameter

$$p = \frac{p(z_j = 1|\mathcal{D}, \beta, z_{-j}, w)}{p(z_j = 0|\mathcal{D}, \beta, z_{-j}, w) + p(z_j = 1|\mathcal{D}, \beta, z_{-j}, w)}. \quad (23)$$

Finally, to sample from $\beta_j^{(i)}$ we use a Metropolis-Hastings within Gibbs step, wherein a proposal $\beta_j^{(i)}$ is sampled from a random-walk proposition kernel K . The proposal is then accepted with probability A or rejected with probability $1 - A$, in which case $\beta_j^{(i)} \leftarrow \beta_j^{(i-1)}$. Noting A is given by,

$$A = \min \left(1, \frac{p(\mathcal{D}; \beta_{-j}, \beta_j^{(i)}, z^{(i)})\pi(\beta_j^{(i)})}{p(\mathcal{D}; \beta_{-j}, \beta_j^{(i-1)}, z^{(i)})\pi(\beta_j^{(i-1)})} \frac{K(\beta_j^{(i-1)}|\beta_j^{(i)})}{K(\beta_j^{(i)}|\beta_j^{(i-1)})} \right) \quad (24)$$

Within our implementation we let $K = N \left(\beta_j^{(i-1)}, \sigma_k^2 \sigma_s^{2(1-z_j^{(i-1)})} \right)$ with $\sigma_k = 0.2$ and $\sigma_s = 10$. The implementation of the sampler is available as an R package that can be installed from <https://github.com/mkomod/survival-ss>.

D Sensitivity analysis

D.1 Sensitivity to starting values

To examine the sensitivity with respect to the initialization of μ , σ and γ we generate data as describe in Section 3.1 taking $(n, p, s, c) = (200, 1000, 10, 0.25)$.

D.1.1 Sensitivity to μ

To examine the sensitivity with respect to initialization of μ we compared four different methods:

- Random: where $\mu_j \stackrel{\text{iid.}}{\sim} N(0, 1)$ for $j = 1, \dots, p$.
- Ridge: where μ is the MLE under the ridge penalty.
- Elastic Net: where μ is the MLE under the elastic net penalty (equal mixture of ridge and LASSO penalties).
- LASSO: where μ is the MLE under the LASSO penalty.

In the last three cases a regularization hyperparameter of $100\lambda_{\min}$ is used, where λ_{\min} is the hyperparameter wherein all estimates coefficients are equal to zero. In order to compute the MLE under the different penalties we use `glmnet`. To evaluate the different initialization methods we compute the ℓ_2 -error, ℓ_1 -error, TPR, FDR, AUC and runtime, presenting the median, lower (5%) and upper (95%) quantiles across 100 runs in Table 6.

Examining Table 6, we notice that within setting 1 the initialization method does not impact the performance of the method with all methods performing equally. It is worth noting the runtime for random initialization is largest, meaning it takes the algorithm longer to converge given a poor initialization. Within settings 2-4, the initialization methods can have a substantial effect on performance. For instance, within settings 3 initialization with ridge yields a median ℓ_2 -error of 1.019, whereas initialization with the LASSO penalty gives a median ℓ_2 -error of 0.394. Furthermore, poor initialization has an effect on the variable selection of the method (Table 6). Overall, initialization of μ using the LASSO gave the best models, obtaining best metrics across the different settings. In some cases however, initialization with the LASSO can be slower than other methods e.g. the elastic net, which produced comparable models.

Setting	Init. Meth.	ℓ_2 -error	ℓ_1 -error	TPR	FDR	AUC	Runtime
<i>Setting 1</i>	Random	0.368 (0.21, 0.70)	0.999 (0.52, 1.86)	1.000 (0.90, 1.00)	0.000 (0.00, 0.00)	1.000 (1.00, 1.00)	19.3s (15.6s,31.3s)
	Ridge	0.368 (0.21, 0.70)	0.999 (0.52, 1.86)	1.000 (0.90, 1.00)	0.000 (0.00, 0.00)	1.000 (1.00, 1.00)	7.1s (4.8s,13.0s)
	Elas. Net.	0.368 (0.21, 0.70)	0.999 (0.52, 1.86)	1.000 (0.90, 1.00)	0.000 (0.00, 0.00)	1.000 (1.00, 1.00)	7.3s (4.5s,12.3s)
	LASSO	0.368 (0.21, 0.70)	1.000 (0.52, 1.86)	1.000 (0.90, 1.00)	0.000 (0.00, 0.00)	1.000 (1.00, 1.00)	13.8s (9.4s,19.8s)
<i>Setting 2</i>	Random	0.848 (0.26, 3.06)	1.988 (0.68, 10.34)	0.900 (0.20, 1.00)	0.000 (0.00, 0.50)	1.000 (0.75, 1.00)	29.3s (19.0s,44.9s)
	Ridge	0.838 (0.26, 3.43)	1.970 (0.69, 11.70)	0.900 (0.30, 1.00)	0.000 (0.00, 0.50)	1.000 (0.74, 1.00)	6.9s (3.0s,12.3s)
	Elas. Net.	0.565 (0.24, 1.72)	1.566 (0.67, 4.58)	1.000 (0.70, 1.00)	0.000 (0.00, 0.15)	1.000 (0.90, 1.00)	7.4s (4.9s,12.2s)
	LASSO	0.445 (0.23, 1.13)	1.204 (0.64, 3.07)	1.000 (0.80, 1.00)	0.000 (0.00, 0.10)	1.000 (0.95, 1.00)	12.3s (8.4s,20.5s)
<i>Setting 3</i>	Random	0.669 (0.21, 3.66)	1.856 (0.58, 12.96)	1.000 (0.30, 1.00)	0.000 (0.00, 0.55)	1.000 (0.75, 1.00)	15.7s (10.4s,26.6s)
	Ridge	1.019 (0.21, 3.58)	2.680 (0.62, 11.69)	0.900 (0.40, 1.00)	0.000 (0.00, 0.33)	0.999 (0.75, 1.00)	8.5s (3.0s,19.1s)
	Elas. Net.	0.423 (0.19, 1.68)	1.170 (0.53, 4.19)	1.000 (0.80, 1.00)	0.000 (0.00, 0.10)	1.000 (0.95, 1.00)	10.6s (6.0s,17.9s)
	LASSO	0.394 (0.18, 1.44)	1.118 (0.53, 3.28)	1.000 (0.90, 1.00)	0.000 (0.00, 0.09)	1.000 (0.95, 1.00)	11.8s (7.0s,19.8s)
<i>Setting 4</i>	Random	0.464 (0.21, 2.88)	1.289 (0.57, 9.30)	1.000 (0.60, 1.00)	0.000 (0.00, 0.33)	1.000 (0.84, 1.00)	17.1s (11.2s,27.4s)
	Ridge	0.562 (0.22, 3.08)	1.562 (0.63, 9.86)	1.000 (0.50, 1.00)	0.000 (0.00, 0.33)	1.000 (0.80, 1.00)	10.9s (4.8s,17.5s)
	Elas. Net.	0.398 (0.19, 1.41)	1.071 (0.50, 3.40)	1.000 (0.90, 1.00)	0.000 (0.00, 0.10)	1.000 (0.95, 1.00)	10.6s (6.8s,17.0s)
	LASSO	0.390 (0.18, 1.15)	1.058 (0.50, 3.05)	1.000 (0.90, 1.00)	0.000 (0.00, 0.10)	1.000 (0.95, 1.00)	12.0s (6.5s,21.3s)

Table 6: Sensitivity to different initialization methods for μ . Presented are the median and (5%, 95%) quantiles. Data is generated taking $(n, p, s, c) = (200, 1000, 10, 0.25)$.

D.1.2 Sensitivity to σ and γ

To examine the sensitivity with respect to σ and γ we performed a grid search examining starting values of $S \times \Gamma$ where $S = \{0.01, 0.05, 0.10, 0.25, 0.5, 0.75, 1.0\}$ and $\Gamma = \{0.01, 0.05, 0.10, 0.25, 0.5, 0.75\}$. To examine the sensitivity we compute and present the mean ℓ_2 -error, ℓ_1 -error, TPR, FDR, AUC and runtime (in seconds) across 100 runs.

Within the simplest setting we notice the method is not sensitive to the starting values, obtaining an ℓ_2 error of 0.41 and ℓ_1 -error of 1.09 and the ideal values for the TPR, FDR and AUC across the different values of σ and γ (Figure 3). More interestingly, the method can be sensitive to the initial values of σ and γ in more complicated settings (settings 2-4). Specifically, when the γ_j s are small the performance is worse than when they are larger (Figures 4 - 6), for instance using a value of $\gamma_j = 0.01, j = 1, \dots, p$, would give a worse performance across all metrics in comparison to a value of $\gamma_j = 0.5$. Furthermore, within setting 2, we notice the performance is sensitive to both the values of σ and γ , with the optimal across all metrics except the FDR given by $\sigma_j = 0.1$ and $\gamma_j = 0.5$ (Figure 4). Finally, for settings 3 and 4 the method is not particularly sensitive to the value of σ , however can be sensitive to the value of γ . Therefore choosing a starting value of γ of at least 0.5 is appropriate within these settings. It is worth pointing out, that in some cases overflow issues were encountered when the values of σ_j and γ_j were too large, for instance when $\gamma_j = 0.75$ and $\sigma_j = 1$.

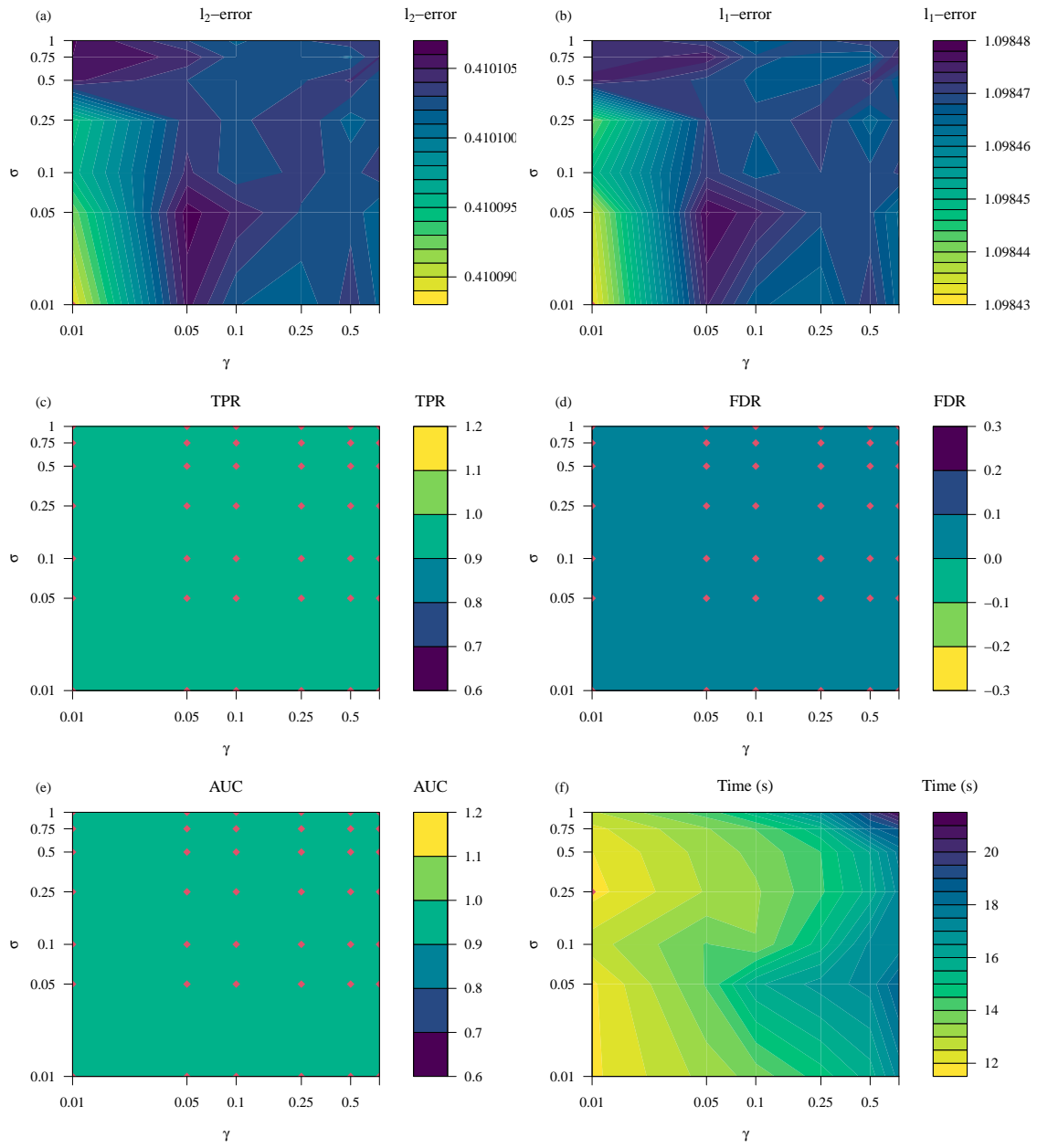


Figure 3: **Setting 1:** sensitivity with respect to σ and γ

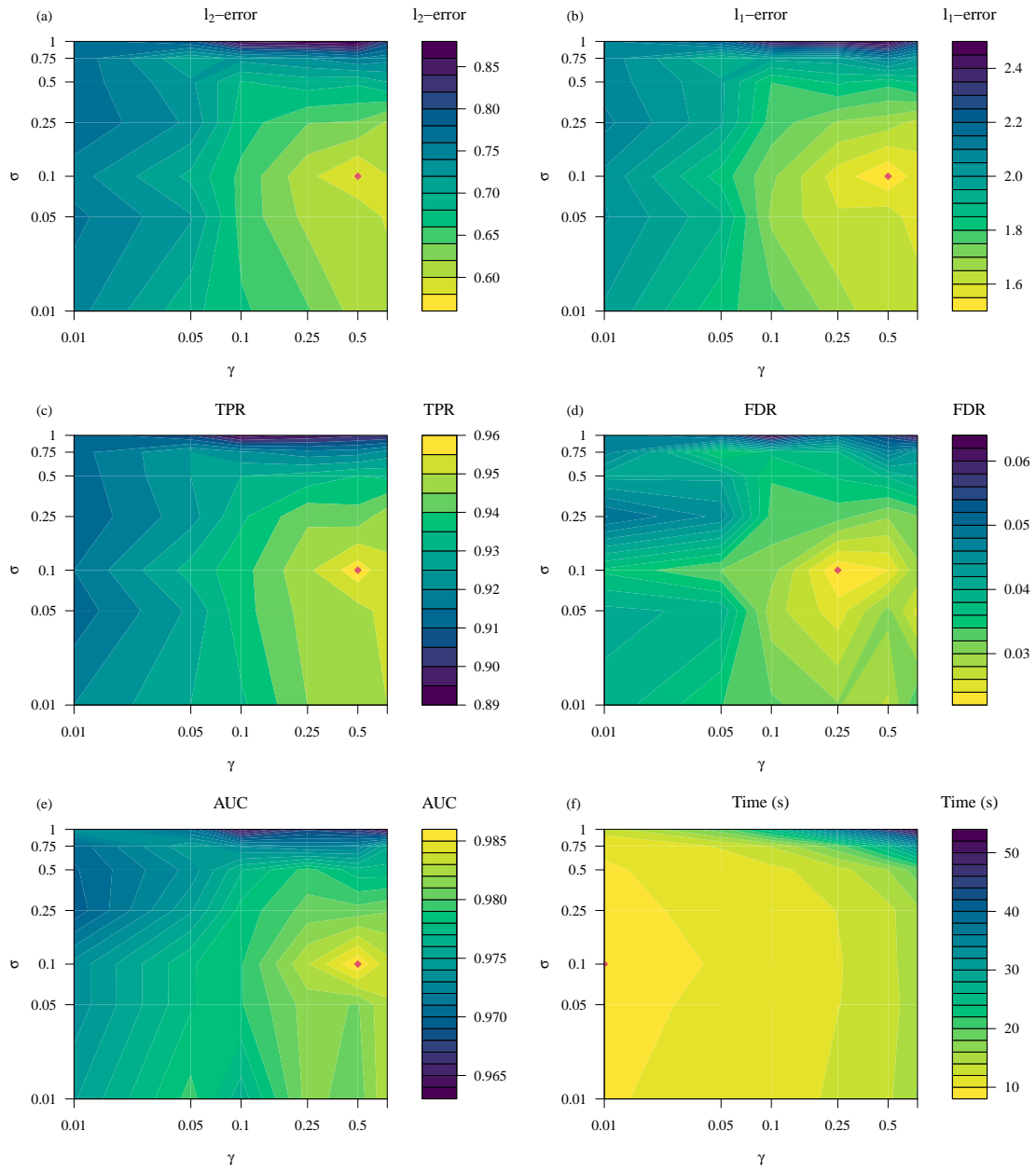


Figure 4: **Setting 2:** sensitivity with respect to σ and γ

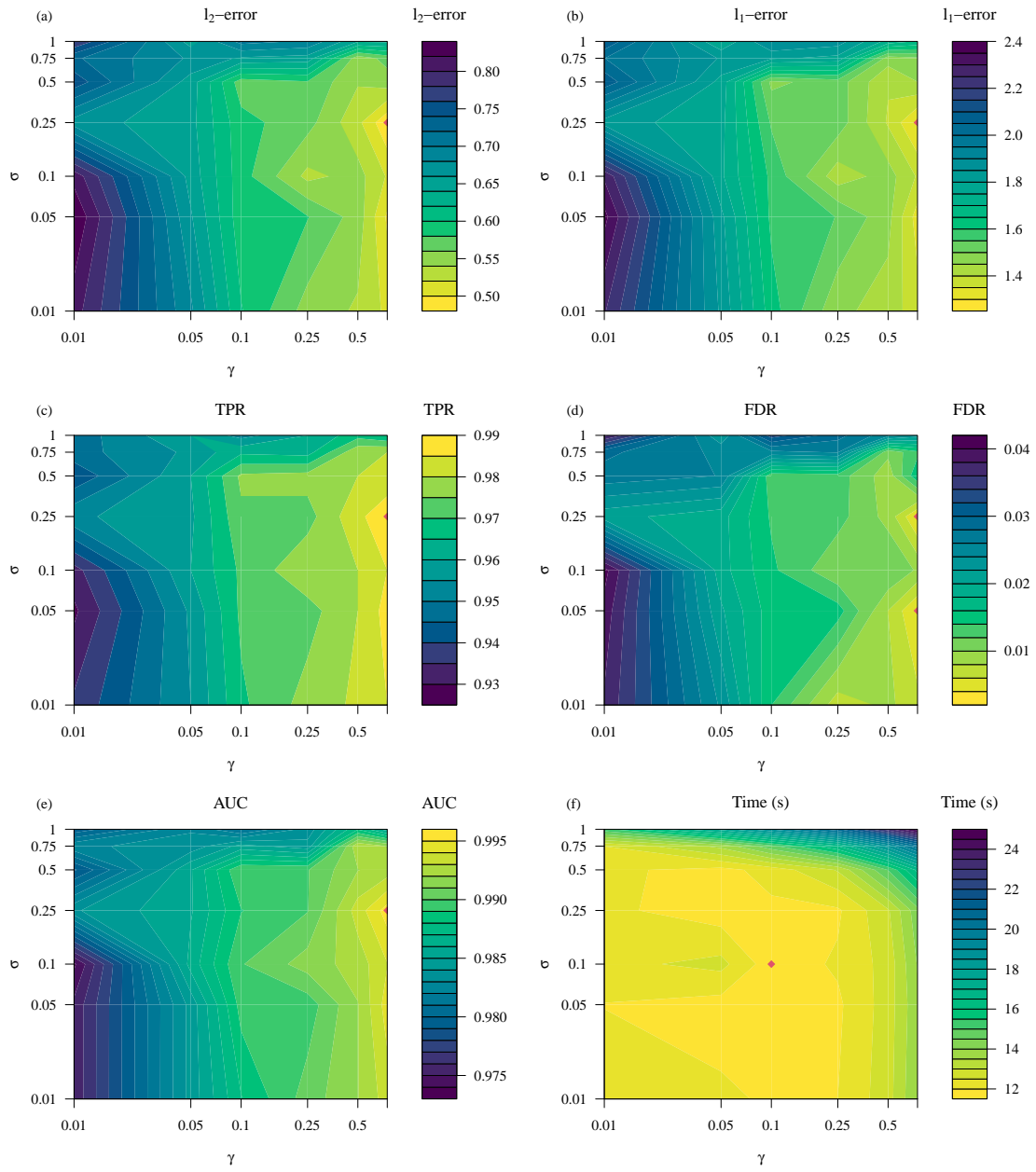


Figure 5: **Setting 3**: sensitivity with respect to σ and γ

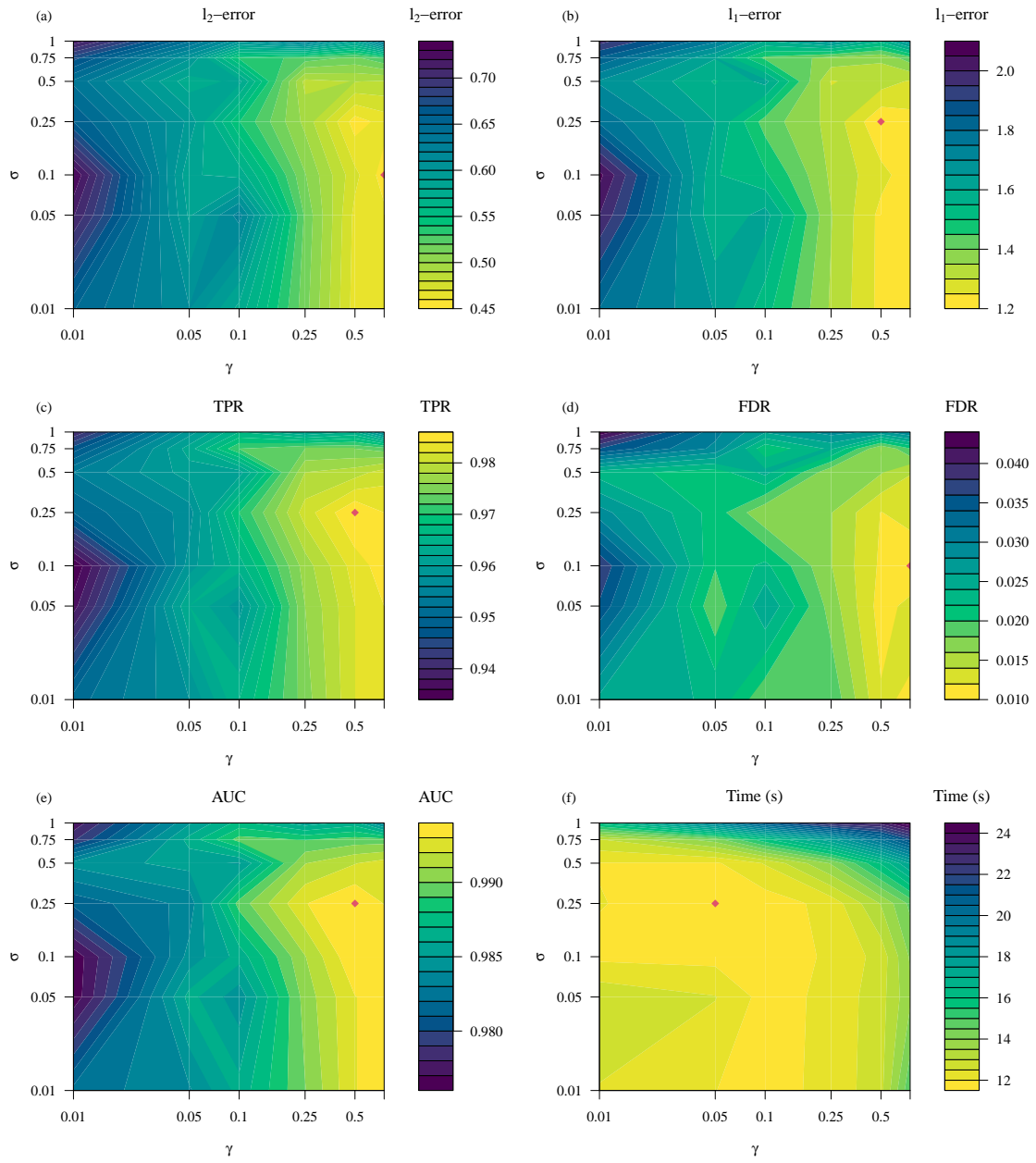


Figure 6: **Setting 4:** sensitivity with respect to σ and γ

D.2 Sensitivity to prior parameters

To evaluate the sensitivity to the prior parameters we ran simulations for Settings 1-4 taking $(n, p, s, c) = (500, 5000, 30, 0.25)$ and fit the VB posterior. To evaluate the performance we compute: (i) ℓ_2 -error, (ii) ℓ_1 -error, (iii) TPR, (iv) FDR, (v) AUC and (vi) runtime (ran on Intel® Xeon® E5-2680 v4 2.40GHz CPUs), reporting the mean across 100 replications. To assess the model's goodness of fit we compute the: (i) ELBO, (ii) ELL under the VB posterior, (iii) c-index, and report the mean across the 100 replications in the following figures.

D.2.1 Sensitivity to λ

We consider a grid of values $\Lambda = \{0.25, 0.5, 1, 2, 4, 8, 10, 20\}$ and fix $a_0 = 1$. For each $\lambda \in \Lambda$ we fit the VB posterior and compute the above performance metrics and goodness of fit measures, reporting the means across 100 replications in Figure 7.

Generally, the proposed method is not particularly sensitive to the value of λ and performs comparably for values between 0.25 and 2, Figure 7 (a)-(e). However, as λ increases there is an increase in the ℓ_2 -error, ℓ_1 -error, meaning the resulting point estimate for β_0 is being overly shrunk, i.e. high prior probability is placed about zero. Further, as λ increases above 10 there is a decrease in TPR and AUC, meaning that fewer features are correctly identified. The decrease in TPR simultaneously leads to an increase in FDR as there are proportionally more incorrectly identified features than correctly identified features. Finally, we note, as λ increases there is a decrease in runtime, Figure 7 (f).

Overall, the ELBO seems to be the most appropriate goodness of fit measure, as it is maximized for model parameter λ that yields the lowest ℓ_2 -error ℓ_1 -error and largest TPR. Within these settings the ELL and c-index do not identify the model with the best performance metric and in turn should be used cautiously.

D.2.2 Sensitivity to a_0

To examine the sensitivity with respect to a_0 , we fix $\lambda = 1$ and examine the grid of values of $A_0 = \{1, 2, 5, 10, 20, 50, 100, 500\}$. For each $a_0 \in A_0$ we compute the VB posterior and report the respective performance metrics and goodness of fit measures (averaged across 100 replications) in Figure 8.

Generally, the proposed method is not particularly sensitive to the value of a_0 , performing equivalently for values between 1 and 100, Figures 8 (a)-(e). However, for large values of a_0 the performance decreases, arising as a large value of a_0 corresponds to us believing *a priori* that many coefficients are non-zero, meaning in the resulting models many coefficients will be non-zero. This behaviour is observed in our results through the increased ℓ_1 -error, ℓ_2 -error and FDR. Finally, as a_0 increases the runtime increases Figure 8 (f).

Regarding goodness of fit measures, the ELBO is maximized for models with correspondingly good performance metrics. Further, the ELL and c-index increase as a_0 increases, meaning models with many non-zero parameters are favoured. These performance metrics should therefore be used cautiously when tuning a_0 .

D.2.3 Sensitivity to λ and a_0

Finally, we consider the sensitivity for both parameters. To do so, we fit the VB posterior for $(\lambda, a_0) \in \Lambda \times A_0$, where Λ and A_0 are the same sets defined earlier. The results for the respective performance metrics and goodness of fit measures are presented in Figures 9 - 12 for settings 1 to 4 respectively.

Generally our method is not sensitive to the hyperparameter values in the simpler settings (1 and 2). For instance, examining Figures 9 and 10 (a) - (e), we notice that the optimal value of the TPR, FDR and AUC is attained for multiple combination of a_0 and λ . Regarding the more complicated settings (3 and 4), our method can be sensitive to λ and a_0 , for instance, in setting 3, poor selection of a_0 and λ can have an impact on the FDR (Figure 11 (d)), in addition, metrics are not consistently optimal for a single combination of λ and a_0 . For example, in setting 3 the optimal value of ℓ_2 -error is obtained when $(\lambda, a_0) = (2, 100)$ whereas the optimal AUC is obtained when $(\lambda, a_0) = (4, 100)$, meaning in practice a trade-off may need to be made between better point estimates and variable selection.

As before, the ELBO seems to be the most appropriate goodness of fit measure for most settings. However, in highly correlated settings, where there is no single “best” parameter values, the optimal ELBO corresponds to the model with smallest ℓ_1 -error [Figures 9 (g) and 12 (g)]. Meaning, other measures are more appropriate if the practitioner wishes to optimise other performance metrics, e.g. the TPR. Finally, the ELL and c-index should be used cautiously as these favour models with many non-zero coefficients and should therefore be used for tuning λ when a_0 is fixed.

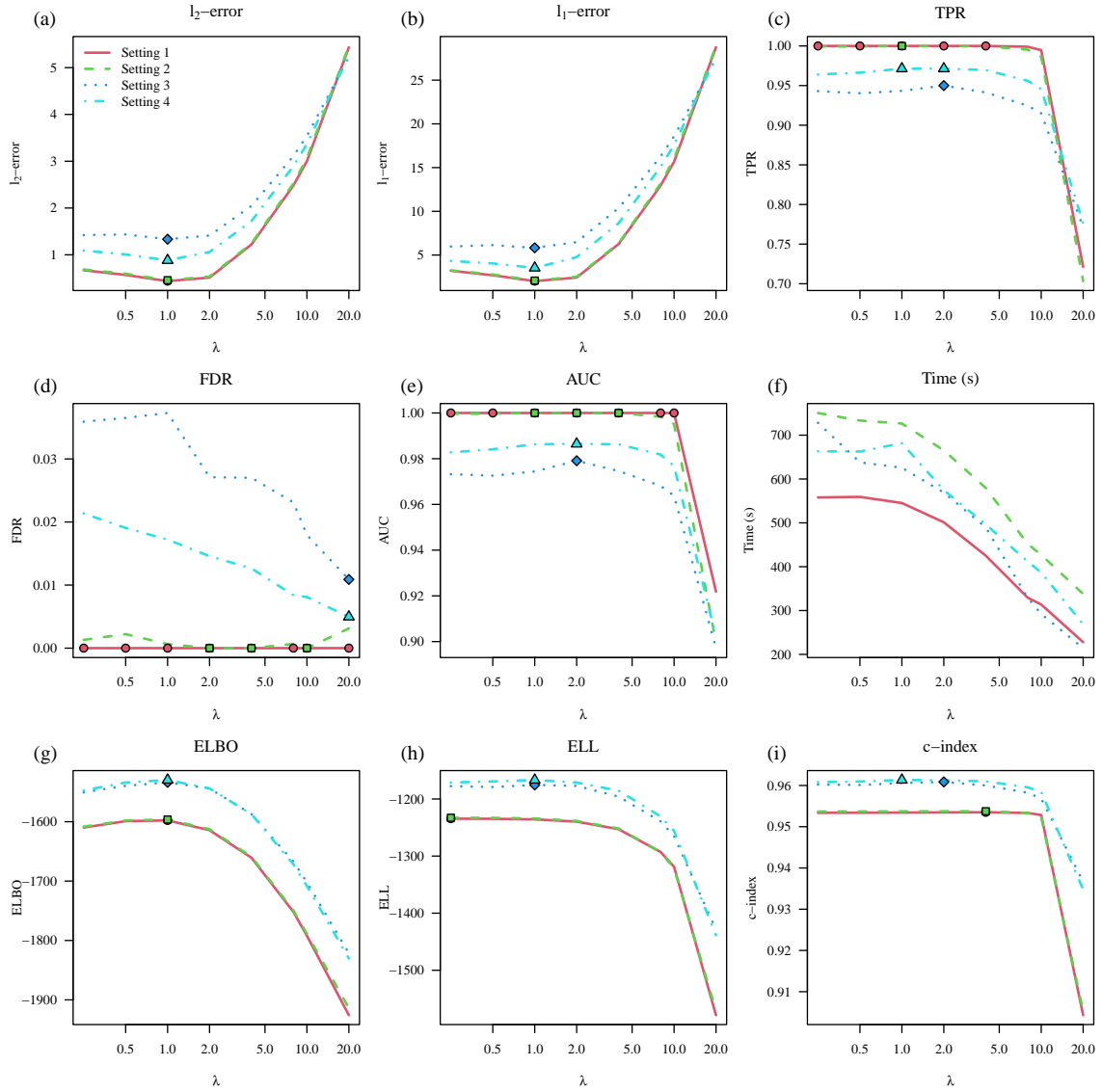


Figure 7: Sensitivity to λ for $a_0 = 1$.

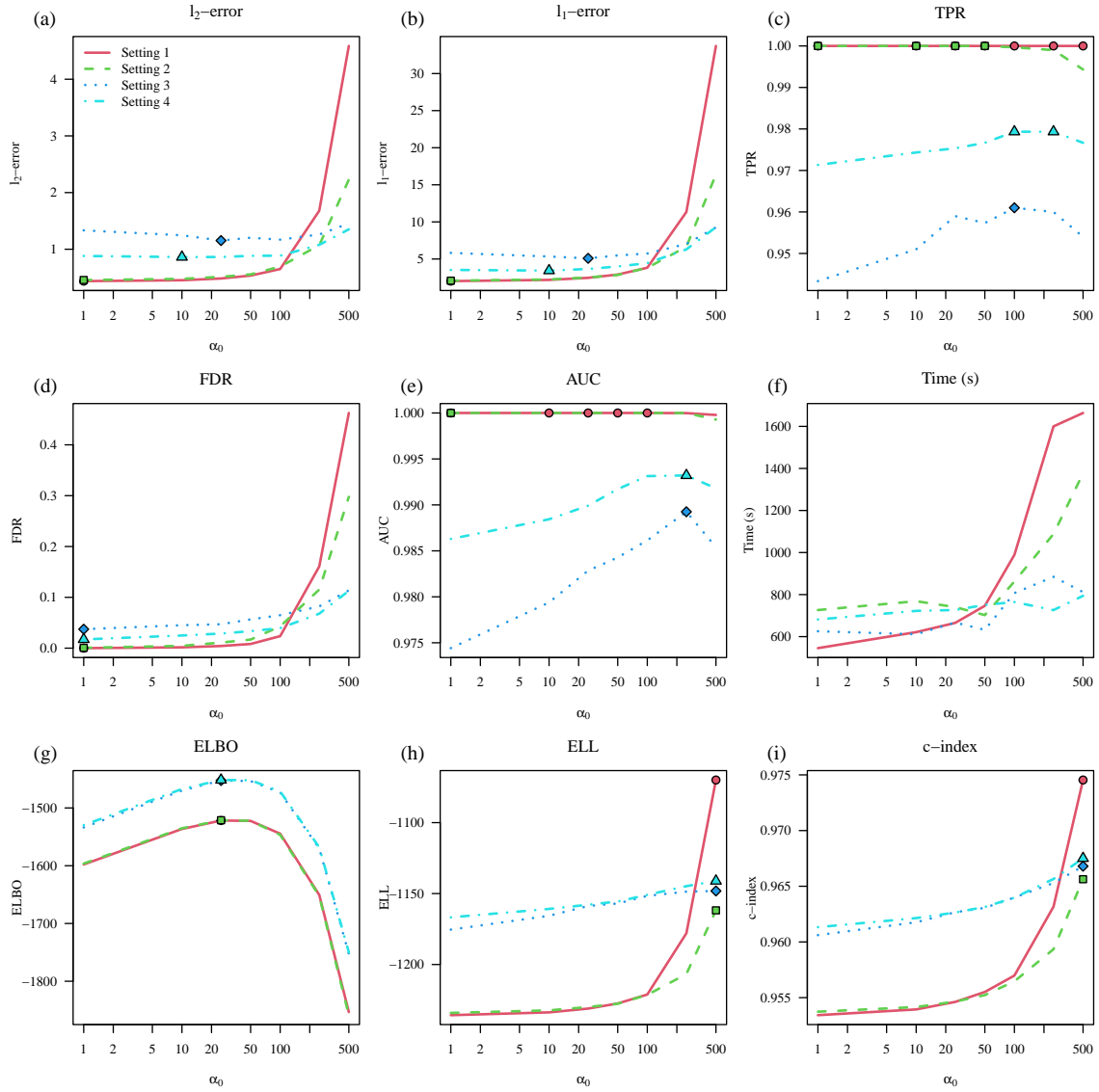


Figure 8: Sensitivity to a_0 for $\lambda = 1$

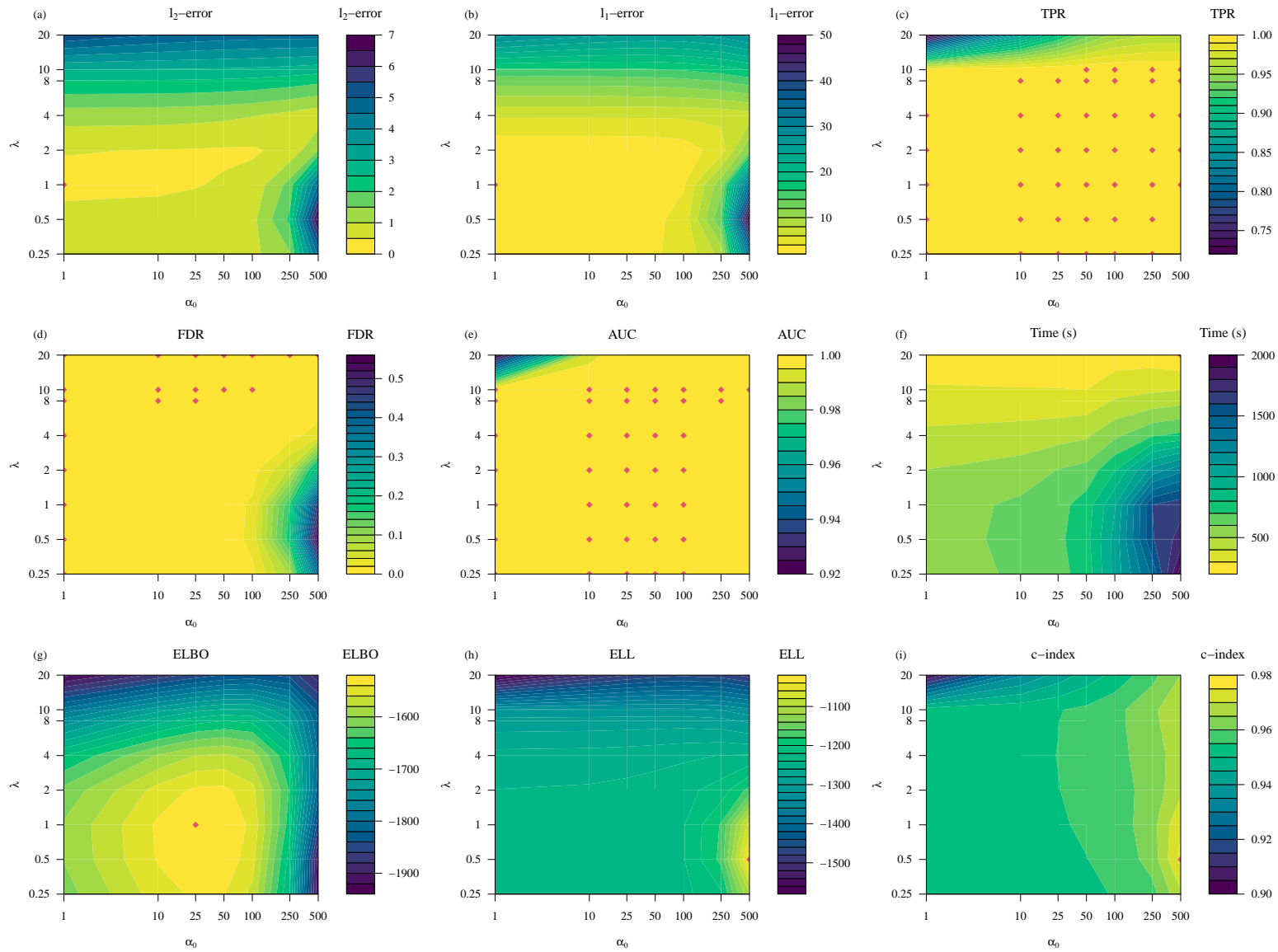


Figure 9: **Setting 1**: sensitivity with respect to λ and α_0 .

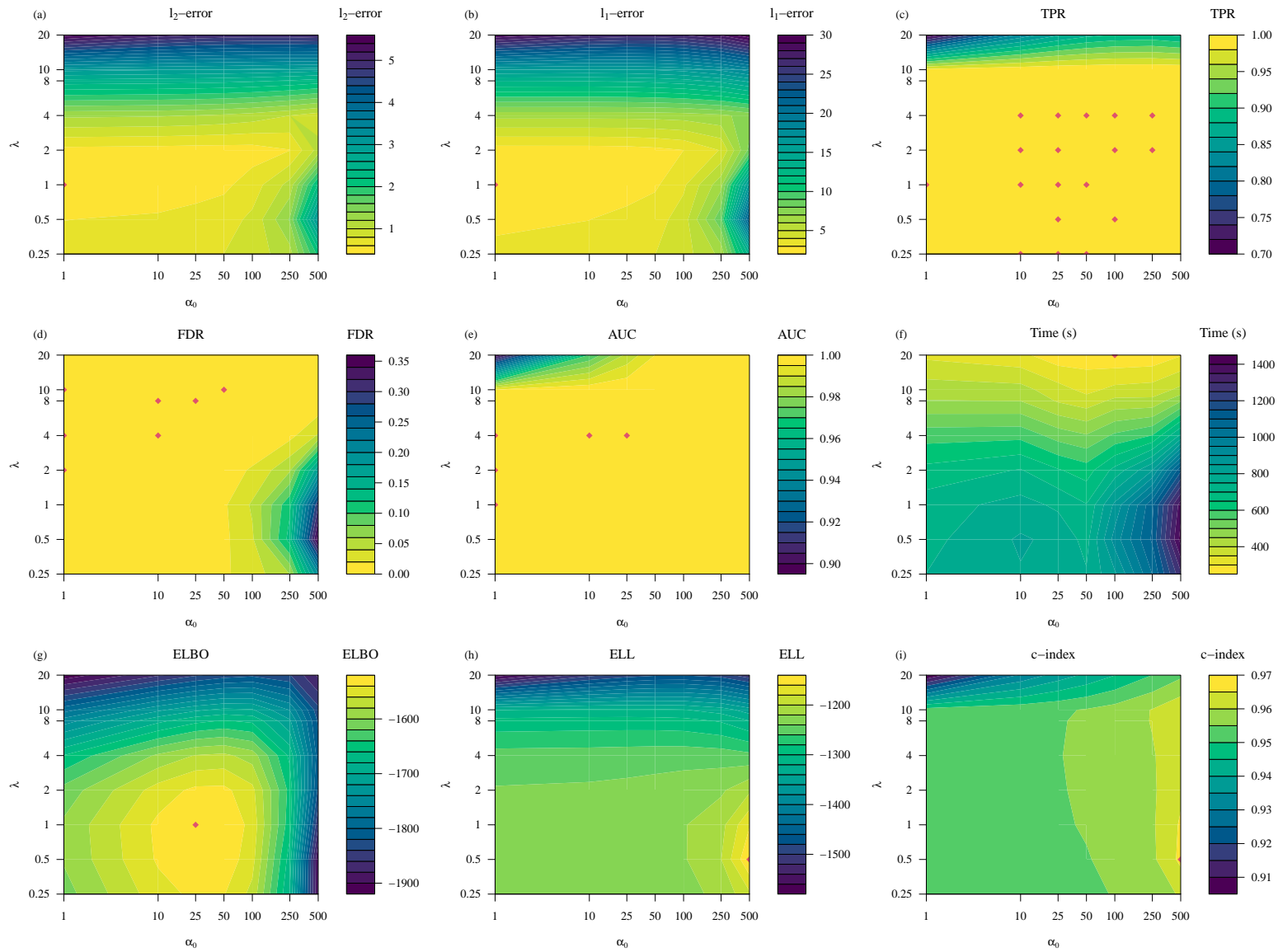


Figure 10: **Setting 2**: sensitivity with respect to λ and α_0 .

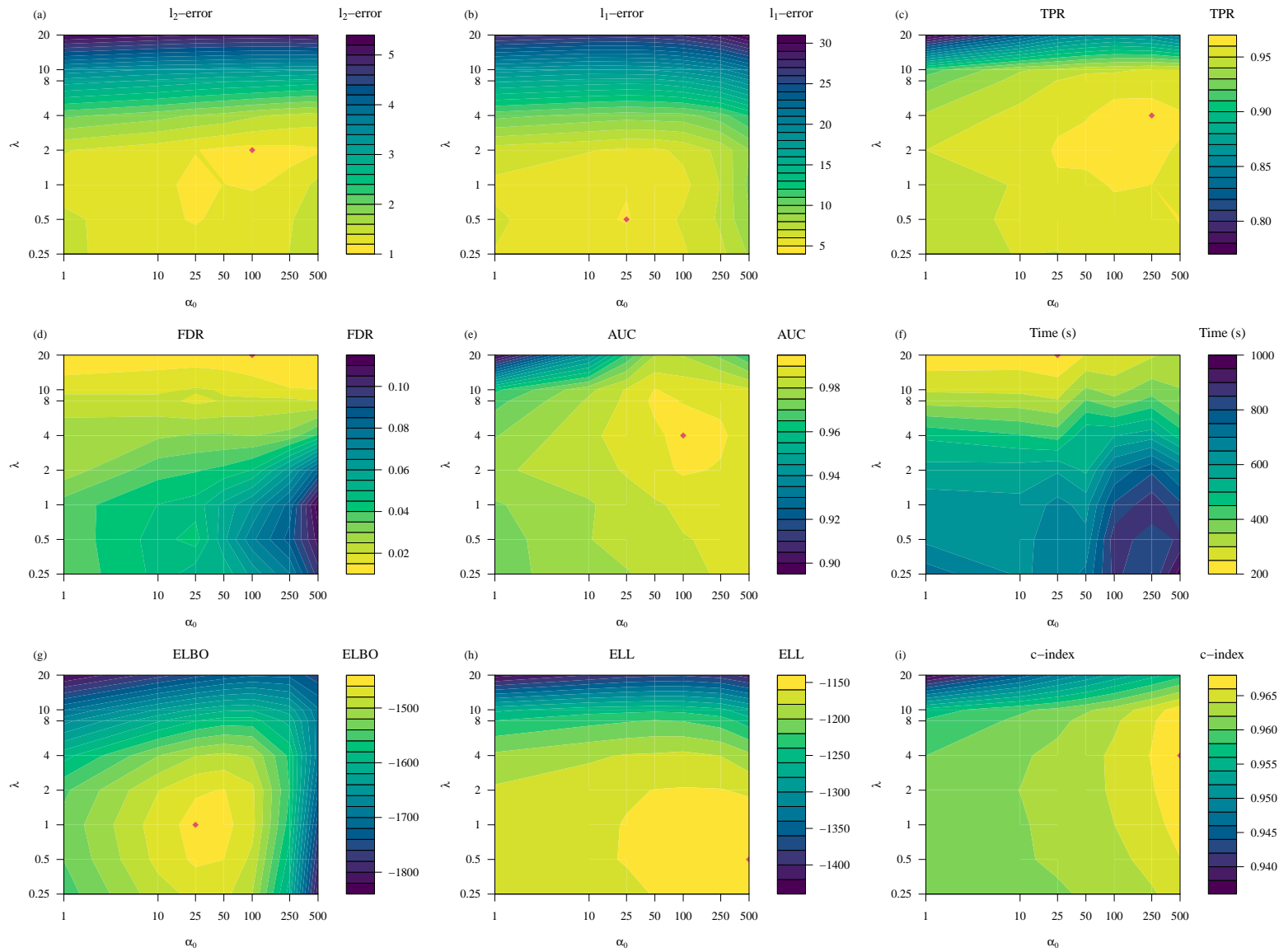


Figure 11: **Setting 3**: sensitivity with respect to λ and α_0 .

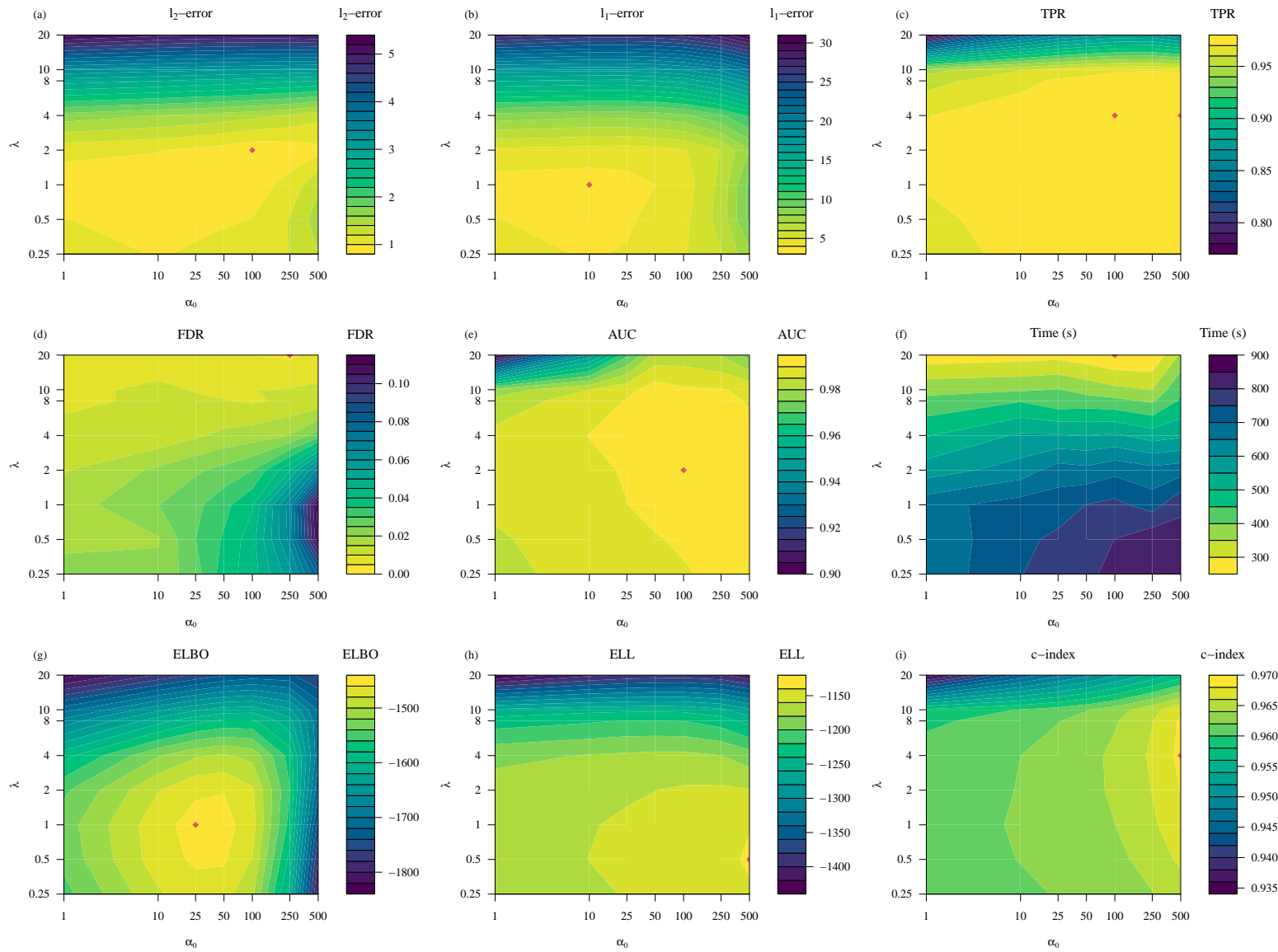


Figure 12: **Setting 4**: sensitivity with respect to λ and α_0 .

E Application to real data

E.1 Availability of datasets

The datasets can be freely downloaded from:

- Ovarian cancer dataset: [https://xenabrowser.net/datapages/?cohort=GDC%20TCGA%20ovarian%20Cancer%20\(OV\)&removeHub=https%3A%2F%2Fxcna.treehouse.gi.ucsc.edu%3A443](https://xenabrowser.net/datapages/?cohort=GDC%20TCGA%20ovarian%20Cancer%20(OV)&removeHub=https%3A%2F%2Fxcna.treehouse.gi.ucsc.edu%3A443)
- Breast cancer dataset: [https://xenabrowser.net/datapages/?cohort=Breast%20Cancer%20\(Yau%202010\)&removeHub=https%3A%2F%2Fxcna.treehouse.gi.ucsc.edu%3A443](https://xenabrowser.net/datapages/?cohort=Breast%20Cancer%20(Yau%202010)&removeHub=https%3A%2F%2Fxcna.treehouse.gi.ucsc.edu%3A443)

E.2 Ovarian cancer dataset

We examine the low and high risk groups constructed using the prognostic index for the ovarian cancer dataset. To construct the groups, we selected the model fit with $\lambda = 0.5$ for the first fold, which has the validation c-index of 0.57, the lowest value obtained across the different values of λ and folds. We chose this value of λ and fold to demonstrate how comparison of groups can highlight outliers and indicate when splitting based on the prognostic index may not be appropriate.

As before, to construct the groups, the validation set was split based on the median value of the prognostic index computed on the training set. The pairwise posterior probability that a patient within the high risk group is at greater risk than a patient within the low risk group is presented in Figure 13. Immediately we notice two patients within each group that may be outliers: patient 2 within the high-risk group and patient 20 within the low-risk group. In the case of patient 2 within the high-risk group, examining the row from left to right we notice the posterior probability is decreasing from around 0.8 to 0.4, meaning that on furthest end, the high-risk patients in the low-risk groups are at greater risk than patient 2. Regarding patient 20 from the low risk group, we notice the posterior probability across the column is lower in comparison to the other patients within the group. Furthermore the mean posterior probability across the column is 0.73, meaning this may be a borderline case between being in the high and low risk group.

E.3 Breast cancer dataset

Convergence diagnostics for the model fit to the breast cancer dataset are presented in Figure 14 for the ovarian and breast cancer datasets respectively. As with the TCGA data we notice the ELBO

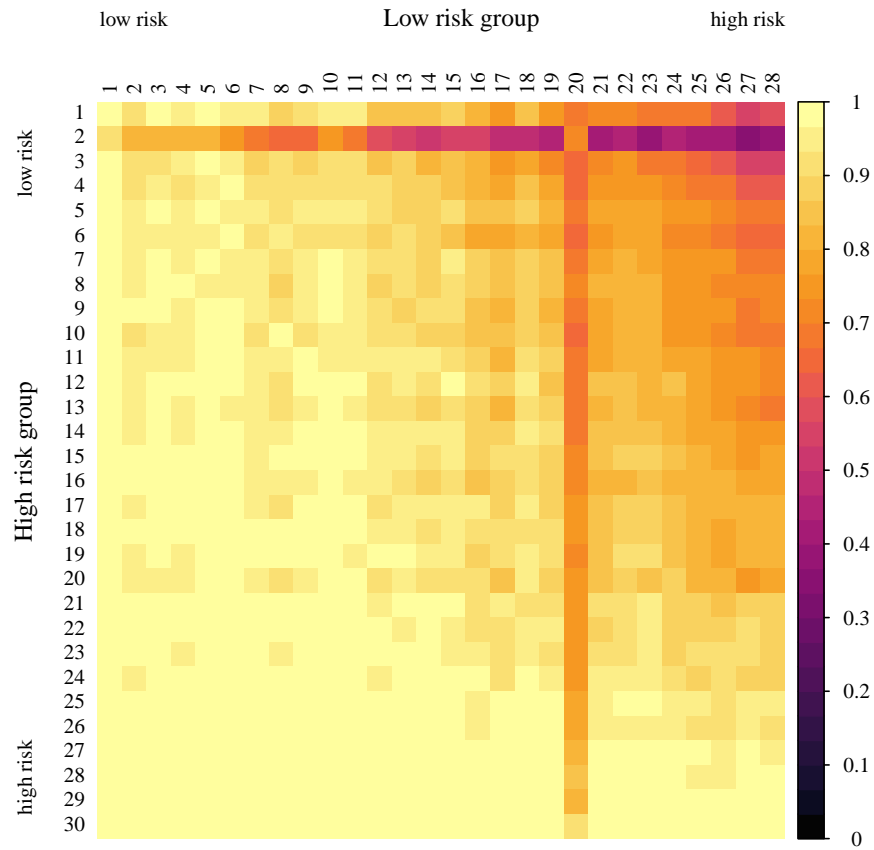


Figure 13: Comparison of validation risk groups for the TCGA ovarian cancer dataset. Rows correspond to patients in the high-risk group and columns to patients in the low-risk group. Both rows and columns are sorted from lowest to highest risk.

is increasing as we iterate the algorithm, suggesting the model fit is improving. Furthermore, we notice that the $\text{KL}(Q\|\Pi)$ is decreasing, suggesting that sparsity is induced. Coupled with the fact the validation expected log-likelihood is increasing, this suggests fewer spurious variables are being selected and the model is fitting better to unseen validation set.

E.4 Model fits

Model fit for different values of λ for the two datasets are presented in Table 7 and Table 8. Reported is the mean and standard deviation across 10 training and validation folds of the: ELBO, ELL, KL, c-index (\hat{k}) and the number of parameters for which $\gamma_j > 0.5$. Examining the different metrics, we notice the model is not particularly sensitivity to the value of λ .

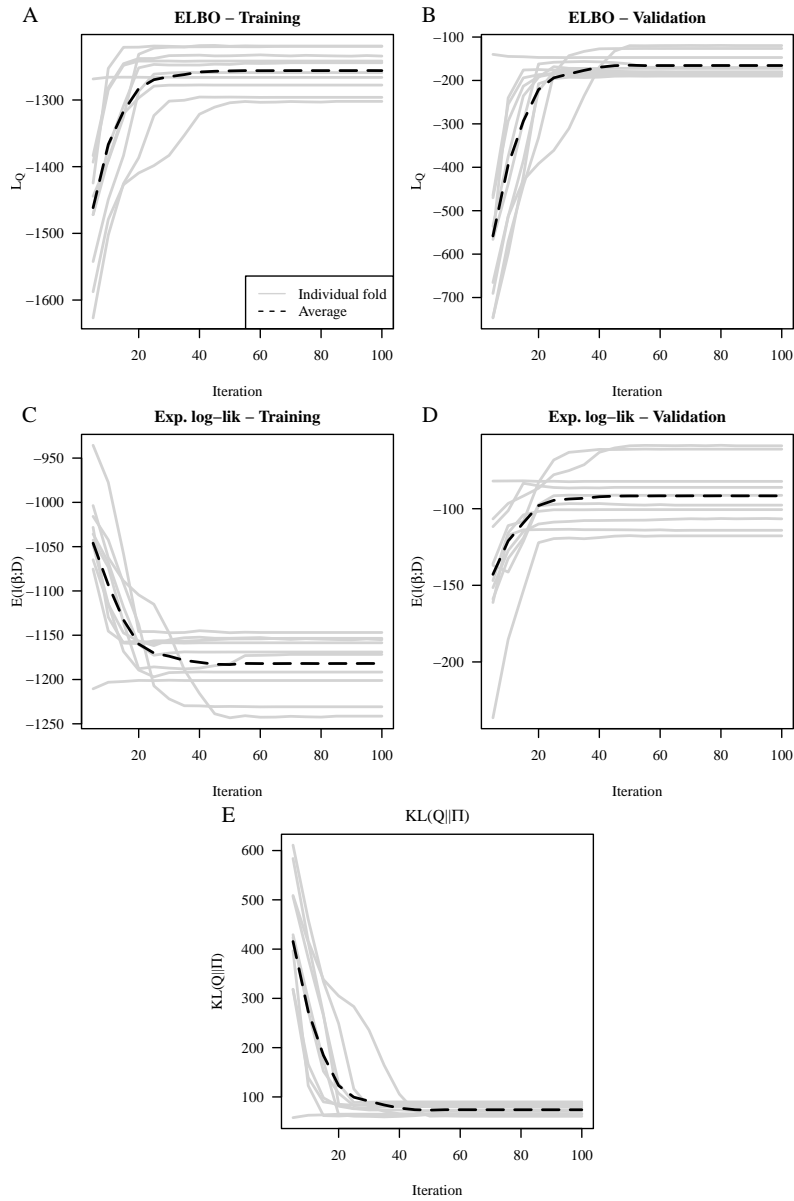


Figure 14: Breast cancer dataset convergence diagnostics for model is fit with $\lambda = 2.5$, Presented is the: ELBO, ELL and KL for the training and validation set. Each fold is presented in (solid) grey, and the mean over the 10 folds presented in (dashed) black. As with the TCGA, we notice as we iterate the model fit improves, fitting better to the unseen validation set.

λ	Training					Validation			
	ELBO	ELL	KL	\hat{k}	$\#\{\gamma > 0.5\}$	ELBO	ELL	KL	\hat{k}
0.05	-1735.7 (21.2)	-1657.5 (26.1)	78.2 (12.2)	0.628 (0.018)	2.0 (1.4)	-189.3 (20.1)	-111.1 (12.3)	78.2 (12.2)	0.558 (0.044)
0.10	-1733.7 (20.6)	-1647.0 (31.9)	86.8 (13.7)	0.646 (0.018)	3.1 (1.7)	-197.8 (24.5)	-111.0 (12.3)	86.8 (13.7)	0.572 (0.041)
0.25	-1795.2 (208.5)	-1604.1 (129.5)	191.1 (333.6)	0.687 (0.085)	15.9 (40.5)	-322.2 (398.1)	-131.1 (65.3)	191.1 (333.6)	0.581 (0.042)
0.50	-1725.8 (21.3)	-1635.1 (30.9)	90.7 (15.1)	0.681 (0.021)	4.3 (2.1)	-202.3 (25.1)	-111.7 (13.0)	90.7 (15.1)	0.588 (0.030)
0.75	-1721.8 (22.4)	-1631.3 (31.2)	90.5 (13.4)	0.695 (0.015)	4.5 (2.0)	-202.8 (24.5)	-112.3 (14.1)	90.5 (13.4)	0.590 (0.050)
1.00	-1719.2 (20.6)	-1620.4 (37.5)	98.8 (26.8)	0.701 (0.023)	6.3 (3.9)	-211.6 (37.3)	-112.8 (13.6)	98.8 (26.8)	0.585 (0.034)
1.25	-1713.7 (22.9)	-1622.7 (27.3)	91.0 (14.1)	0.703 (0.016)	5.5 (2.2)	-204.7 (21.0)	-113.7 (14.0)	91.0 (14.1)	0.594 (0.037)
1.50	-1712.8 (22.9)	-1620.3 (28.4)	92.4 (15.0)	0.706 (0.015)	6.1 (2.4)	-205.4 (24.8)	-113.0 (14.5)	92.4 (15.0)	0.587 (0.043)
1.75	-1709.9 (20.8)	-1625.1 (29.9)	84.9 (12.0)	0.704 (0.014)	5.2 (1.9)	-197.7 (24.0)	-112.8 (14.5)	84.9 (12.0)	0.605 (0.044)
2.00	-1707.6 (21.7)	-1618.2 (28.5)	89.4 (13.1)	0.717 (0.021)	6.1 (2.0)	-202.8 (22.7)	-113.4 (14.1)	89.4 (13.1)	0.589 (0.038)
2.50	-1704.5 (22.9)	-1620.3 (28.7)	84.2 (9.1)	0.717 (0.011)	5.8 (1.5)	-198.1 (22.7)	-113.9 (16.1)	84.2 (9.1)	0.610 (0.054)
3.00	-1702.5 (21.7)	-1623.2 (31.2)	79.3 (10.6)	0.715 (0.014)	5.5 (1.8)	-191.2 (23.7)	-111.9 (13.7)	79.3 (10.6)	0.606 (0.034)
4.00	-1695.7 (21.9)	-1626.0 (28.8)	69.6 (10.7)	0.713 (0.011)	4.8 (1.8)	-181.4 (20.5)	-111.7 (13.2)	69.6 (10.7)	0.602 (0.021)
5.00	-1693.9 (21.4)	-1629.1 (25.9)	64.7 (8.7)	0.713 (0.012)	4.4 (1.3)	-176.3 (19.4)	-111.5 (13.6)	64.7 (8.7)	0.605 (0.045)

Table 7: **Ovarian cancer dataset**, model fit for different values of λ

λ	Training					Validation			
	ELBO	ELL	KL	\hat{k}	$\#\{\gamma > 0.5\}$	ELBO	ELL	KL	\hat{k}
0.05	-1284.1 (29.8)	-1216.9 (28.9)	67.1 (1.6)	0.693 (0.009)	2.0 (0.0)	-155.1 (18.1)	-87.9 (19.0)	67.1 (1.6)	0.625 (0.039)
0.10	-1282.2 (29.8)	-1210.6 (30.9)	71.6 (7.3)	0.706 (0.010)	2.6 (1.0)	-161.1 (22.9)	-89.5 (20.2)	71.6 (7.3)	0.615 (0.071)
0.25	-1278.9 (29.5)	-1199.7 (31.2)	79.3 (12.3)	0.729 (0.019)	4.1 (1.8)	-170.6 (24.7)	-91.4 (19.7)	79.3 (12.3)	0.598 (0.071)
0.50	-1274.6 (29.1)	-1189.3 (34.9)	85.3 (14.9)	0.746 (0.013)	5.4 (2.1)	-176.8 (29.6)	-91.6 (20.8)	85.3 (14.9)	0.615 (0.075)
0.75	-1270.2 (29.2)	-1189.0 (29.8)	81.2 (9.4)	0.752 (0.011)	5.1 (1.6)	-174.1 (22.9)	-92.9 (20.4)	81.2 (9.4)	0.593 (0.081)
1.00	-1268.4 (30.5)	-1187.8 (28.5)	80.6 (12.0)	0.760 (0.012)	5.2 (2.1)	-173.8 (22.5)	-93.2 (21.0)	80.6 (12.0)	0.603 (0.083)
1.25	-1264.1 (29.2)	-1184.0 (30.8)	80.0 (11.3)	0.768 (0.009)	5.4 (2.0)	-173.8 (24.2)	-93.8 (20.3)	80.0 (11.3)	0.590 (0.075)
1.50	-1262.9 (29.6)	-1181.5 (32.4)	81.3 (11.0)	0.772 (0.010)	5.8 (1.8)	-174.8 (25.4)	-93.4 (20.8)	81.3 (11.0)	0.596 (0.064)
1.75	-1260.9 (29.4)	-1179.0 (32.6)	81.9 (15.9)	0.776 (0.012)	6.2 (2.7)	-175.8 (27.6)	-93.9 (20.6)	81.9 (15.9)	0.597 (0.064)
2.00	-1259.1 (29.5)	-1180.6 (32.6)	78.5 (11.0)	0.775 (0.009)	5.7 (1.8)	-172.6 (25.0)	-94.1 (20.5)	78.5 (11.0)	0.584 (0.077)
2.50	-1255.9 (29.5)	-1181.9 (33.3)	74.0 (10.1)	0.777 (0.009)	5.3 (1.6)	-165.6 (25.5)	-91.6 (20.1)	74.0 (10.1)	0.626 (0.075)
3.00	-1252.8 (29.5)	-1184.1 (30.1)	68.7 (8.7)	0.781 (0.005)	4.8 (1.6)	-161.6 (22.0)	-92.9 (19.6)	68.7 (8.7)	0.612 (0.072)
4.00	-1249.3 (29.7)	-1183.1 (31.1)	66.2 (7.7)	0.785 (0.004)	4.9 (1.4)	-158.6 (23.1)	-92.4 (20.2)	66.2 (7.7)	0.619 (0.072)
5.00	-1246.6 (28.7)	-1185.8 (31.4)	60.8 (9.4)	0.787 (0.008)	4.5 (1.8)	-153.2 (24.8)	-92.4 (20.2)	60.8 (9.4)	0.610 (0.069)

Table 8: **Breast cancer dataset**, model fit for different values of λ